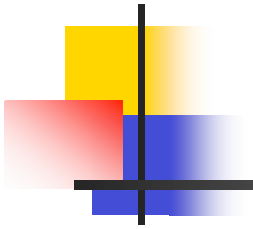

Nanoparticles, nanorods, nanowires

- Nanoparticles, nanocrystals, nanospheres, quantum dots, etc.
  - Drugs, proteins, etc.
- Nanorods, nanowires.
- Optical and electronic properties.
- Organization using biomolecules.
- Future possibilities.

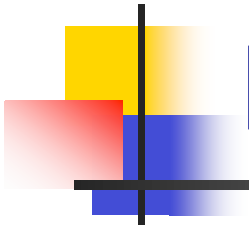

Nanoparticles

- Materials: QDs, magnets, noble metals
- Synthesis
  - Reduction of metal salt
  - Production of insoluble salt
  - Micelle confinement
  - Microbial production
  - Biomolecular nucleation
- Control of: composition, size, shape, crystal structure, and surface chemistry.
- Properties: Optical, electrical, physical, chemical

Nanoparticles, gold

- Synthesis
  - Reduction of metal salt

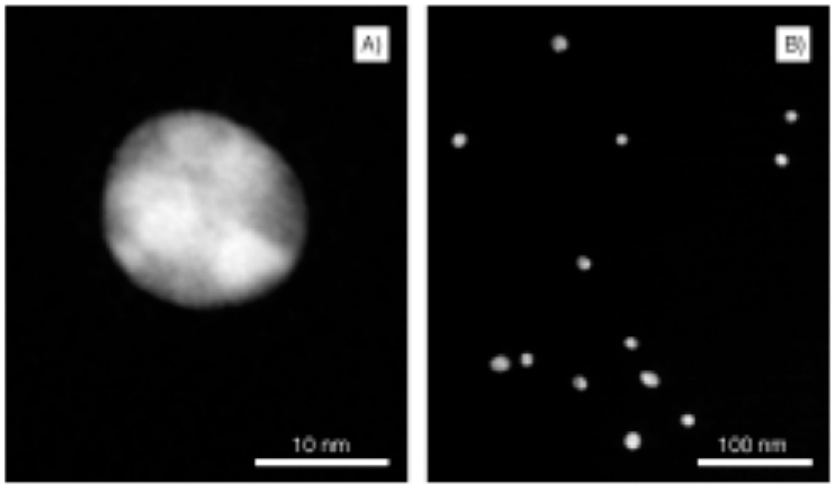

Figure 2. *Gold nanoparticles synthesized by citrate reduction. A) A single particle at high magnification shows its highly spherical shape. B) A region of single nanoparticles at a lower magnification shows the monodispersity of particle sizes.*

Table 1. *The dependence of nanoparticle diameter on citrate concentration in the reductive synthesis of gold nanoparticles.*[a]

Citrate solution added[b] [mL]	Diameter[c] [nm]
1.0	16
0.75	25
0.5	41
0.3	72
0.21	98
0.16	147

[a] Data is taken from reference 34. [b] Trisodium citrate (1% aqueous solution) was added to 50 mL refluxing solution of 0.01% $H[AuCl_4]$. [c] Particle diameters were measured by SEM.

NATURE | VOL 425 | 2 OCTOBER 2003 |

Nanoparticles, silver

- Light dependent synthesis

Controlling anisotropic nanoparticle growth through plasmon excitation

Rongchao Jin, Y. Charles Cao, Encai Hao, Gabriella S. Métraux, George C. Schatz & Chad A. Mirkin

Department of Chemistry and Institute for Nanotechnology, Northwestern University, Evanston, Illinois 60208, USA

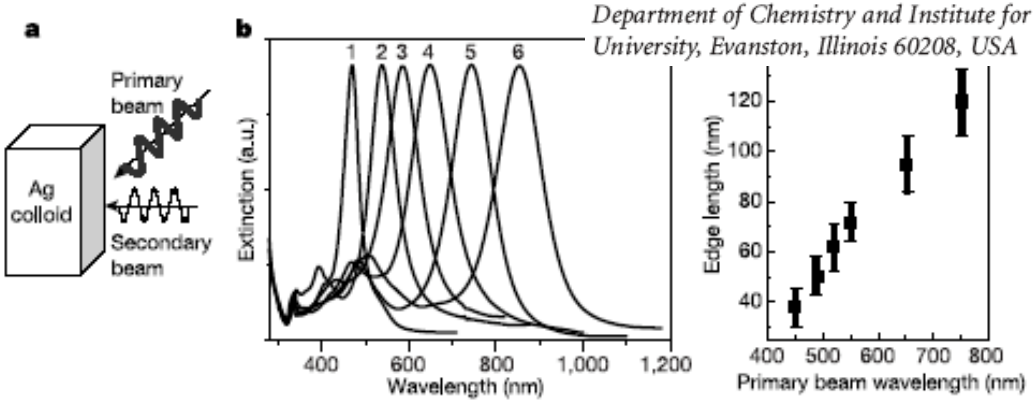

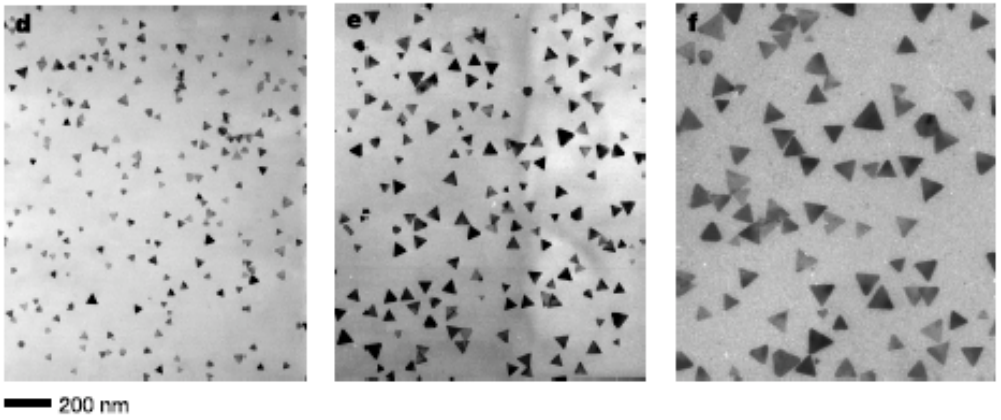

Nanoparticles, organization

Three-dimensional binary superlattices of magnetic nanocrystals and semiconductor quantum dots

F. X. Redl*†, K.-S. Cho*‡, C. B. Murray* & S. O'Brien†

** IBM, T. J. Watson Research Center, Nanoscale Materials and Devices, 1101 Kitchawan Road, Route 134, Yorktown Heights, New York 10598, USA*
† Department of Applied Physics & Applied Mathematics, Columbia University, 200 SW Mudd Building, 500 West 120th Street, New York, New York 10027, USA
‡ Advanced Materials Research Institute (AMRI), University of New Orleans, New Orleans, Louisiana, 70148, USA

NATURE | VOL 423 | 26 JUNE 2003 |

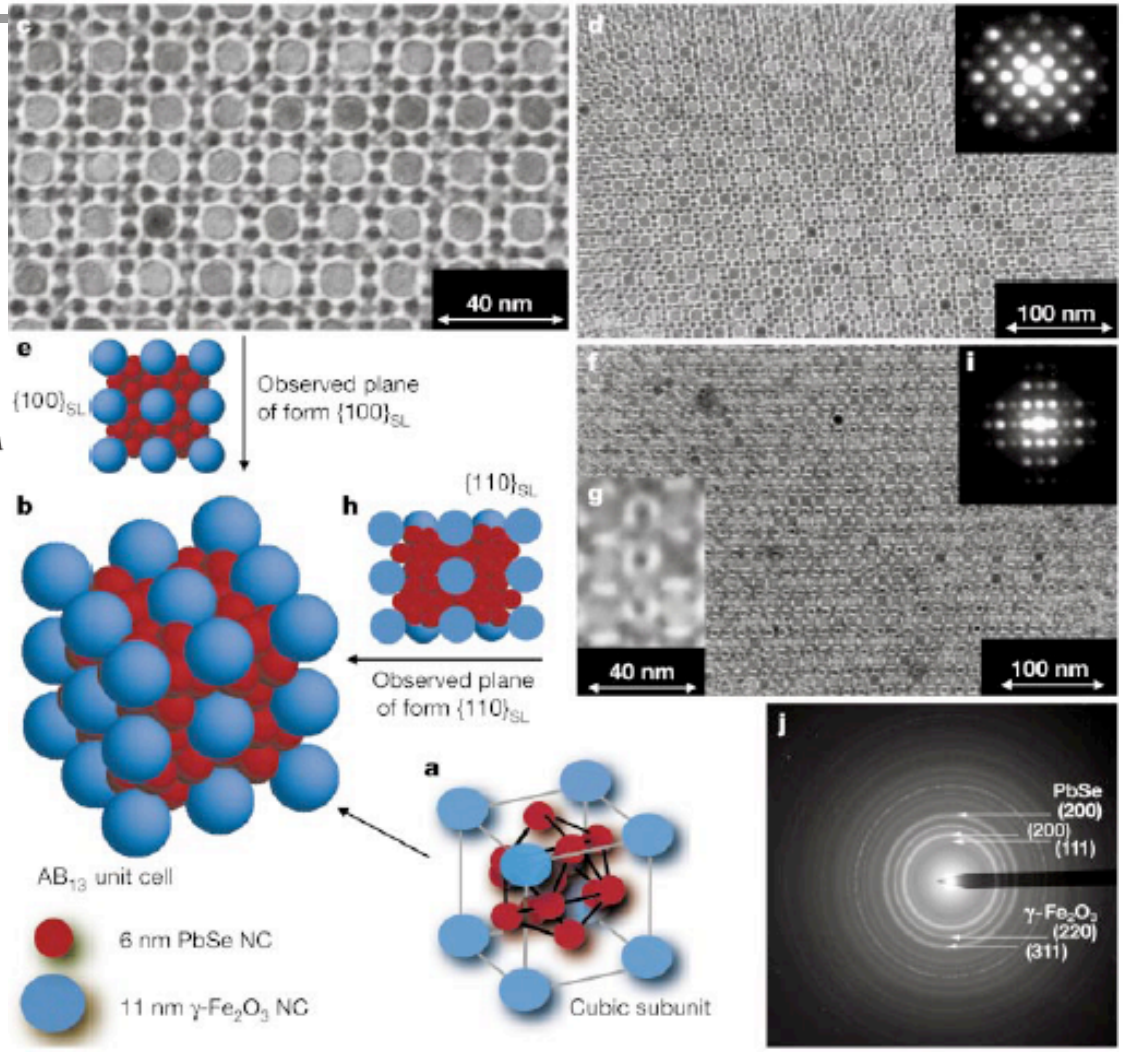

QD Rainbow

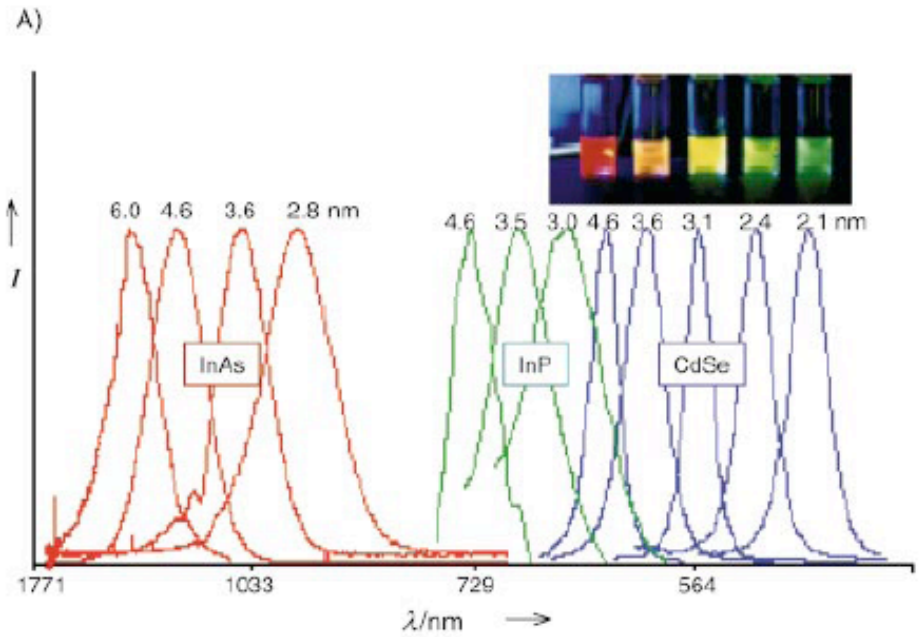

M. Bruchez, Jr., M. Moronne, P. Gin, S. Weiss, A. P. Alivisatos, *Science* **1998**, *281*, 2013–2015.

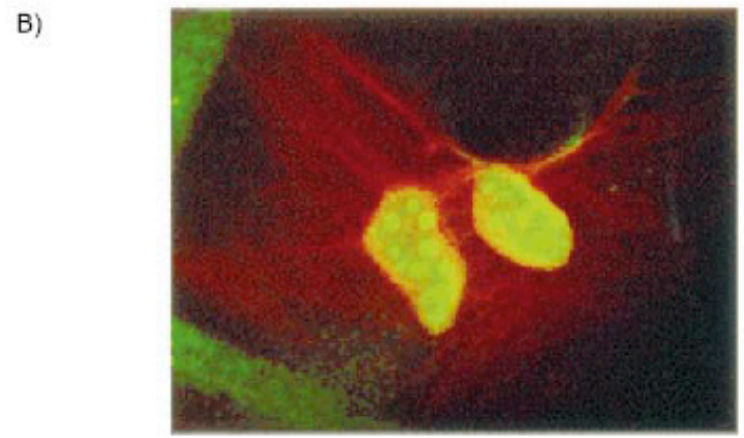

Figure 22. A) Fluorescence emission spectra of semiconductor quantum dots; B) cross-section through dual-labeled mouse fibroblasts. The actin fibers are stained red. The nonspecific labeling of the nuclear membrane by both the red and the green probes results in a yellow color. Reproduced from ref. [17], with permission. Copyright 1998 American Association for the Advancement of Science.

Nanowires

[a] Electrochemical deposition
[b] Vapor-liquid-solid growth
[c] Chemical vapor deposition
[d] Organometallic chemical vapor deposition

- ECD (dc, ac, pulsed)
  - Polycrystalline wires (some single-crystal)
- Pressure injection into template pores.
  - Single-crystal wires

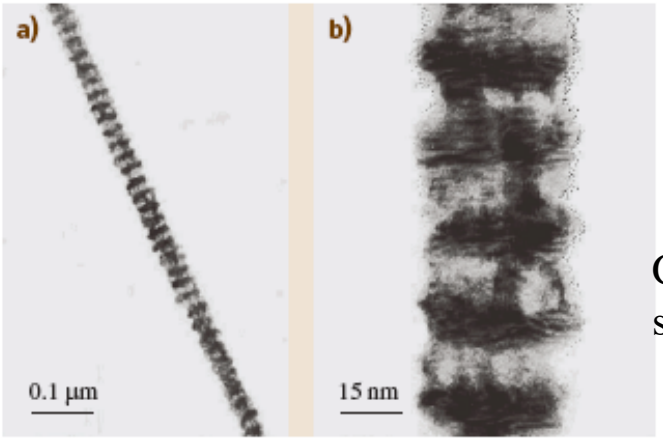

Fig. 4.4 (a) TEM image of a single Co(10 nm)/Cu(10 nm) multilayered nanowire. (b) A selected region of the sample at high magnification [4.76]

Co/Cu layers from one solution by switching cathodic potential.

Material	Growth Technique
Ag	DNA-template, redox template, pulsed ECD[a]
Au	template, ECD[a]
Bi	stress-induced template, vapor-phase template, ECD[a] template, pressure-injection
Bi_2Te_3	template, dc ECD[a]
CdS	liquid-phase (surfactant), recrystalli template, ac ECD[a]
CdSe	liquid-phase (surfactant), redox template, ac ECD[a]
Cu	vapor deposition template, ECD[a]
Fe	template, ECD[c] shadow deposition
GaN	template, CVD[c] VLS[b]
GaAs	template, liquid/vapor OMCVD[d]
Ge	high-T, high-P liquid-phase, redox VLS[b] oxide-assisted
InAs	template, liquid/vapor OMCVD[d]
InP	VLS[b]
Mo	step decoration, ECD[a]+ redox
Ni	template, ECD[a]
PbSe	liquid phase
Pd	step decoration, ECD[a]
Se	liquid-phase, recrystallization template, pressure injection
Si	VLS[b] laser-ablation VLS[b] oxide-assisted low-T VLS[b]
Zn	template, vapor-phase template, ECD[a]
ZnO	VLS[b] template, ECD[a]

Nanowires

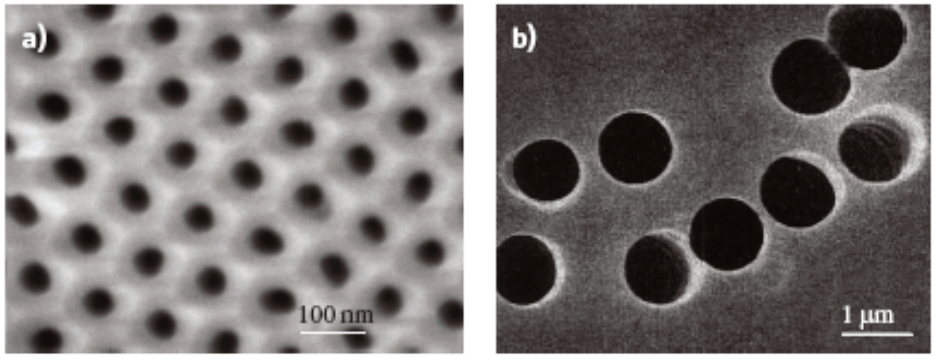

a) Anodic alumina from acid anodized Al film to give hexagonal array of cylindrical holes. b) particle track-etched polycarbonate membrane.

- Templates
  - anodic alumina (Al_2O_3), nano-channel glass, ion track-etched polymers, and mica films.
  - 10-200 nm diameter pores.
  - CNT in templates and as templates.

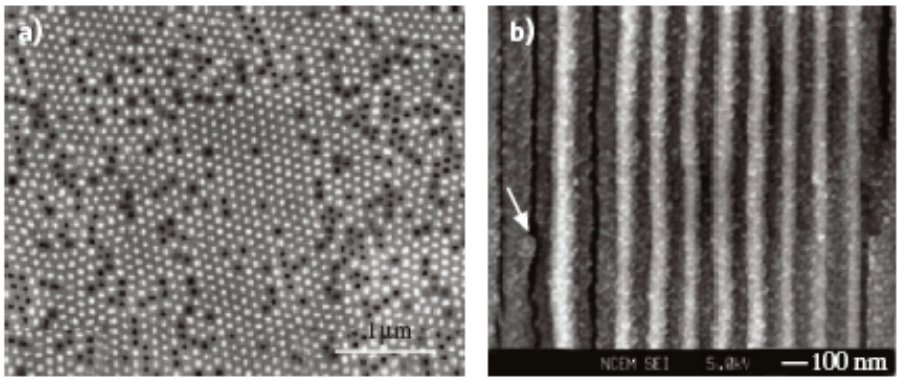

Fig. 4.3 (a) SEM image of a Bi_2Te_3 nanowire array in cross section showing a relatively high pore filling factor. (b) SEM image of a Bi_2Te_3 nanowire array composite along the wire axis [4.34]

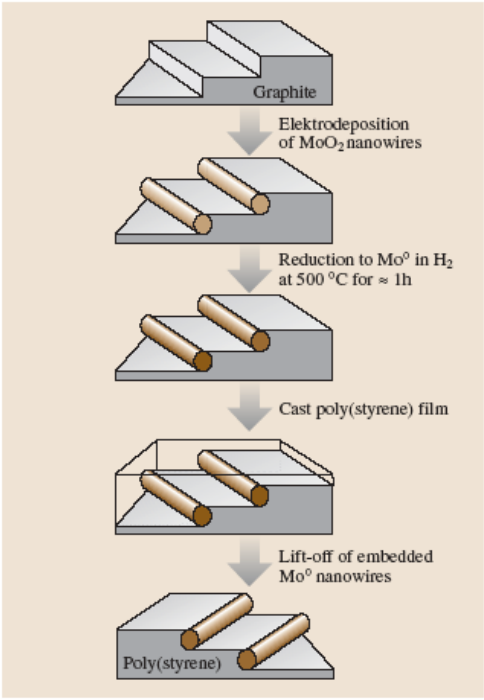

Fig. 4.8 Schematic of the electrodeposition step edge decoration of HOPG (highly oriented pyrolytic graphite) for the synthesis of molybdenum nanowires [4.53, 102]

Protein templates

(also CNT synth, catalyst)

W. Shenton, T. Douglas, M. Young, G. Stubbs, S. Mann, *Adv. Mater.* **1999**, *11*, 253–256.

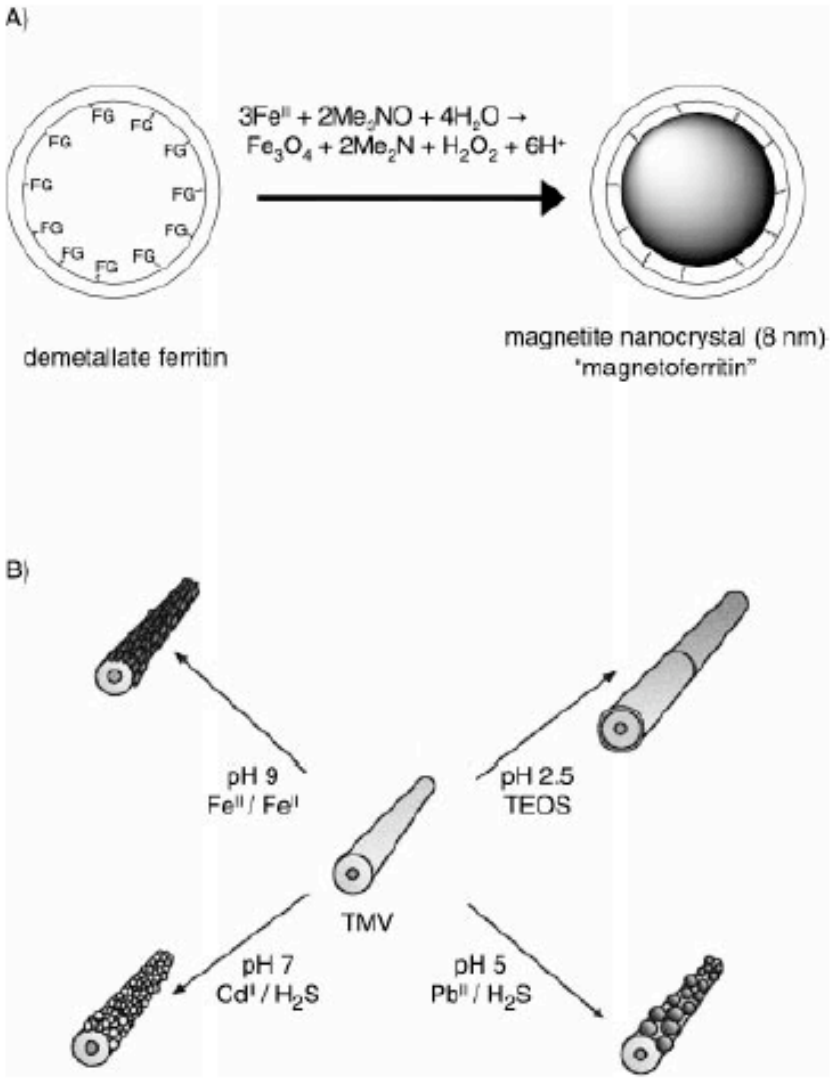

Figure 17. A) Hollow protein cages used as spatially confined bioreactors for the growth of inorganic nanoparticles (FG = functional group, which acts as a nucleation site for biomineralization). B) Synthesis of nanotube composites by using TMV templates. (TEOS = tetraethoxysilane). Reproduced from ref. [144], with permission.

Nanowires

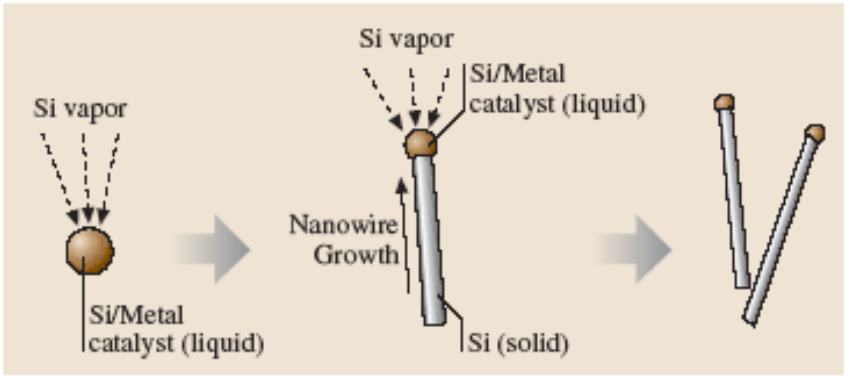

Fig. 4.5 Schematic diagram illustrating the growth of silicon nanowires by the VLS mechanism

- VLS - vapor, liquid, solid
  - Mechanism first proposed for single-crystal Si whisker synthesis (molten Au catalyst).
  - Anisotropic crystal growth.

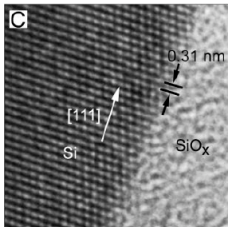

208 SCIENCE • VOL. 279 • 9 JANUARY 1998

A Laser Ablation Method for the Synthesis of Crystalline Semiconductor Nanowires

Alfredo M. Morales and Charles M. Lieber*

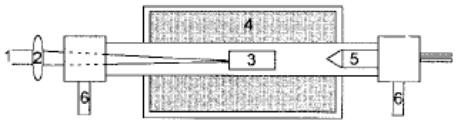

Fig. 1. Schematic of the nanowire growth apparatus. The output from a pulsed laser (1) is focused (2) onto a target (3) located within a quartz tube; the reaction temperature is controlled by a tube furnace (4). A cold finger (5) is used to collect the product as it is carried in the gas flow that is introduced (6, left) through a flow controller and exits (6, right) into a pumping system.

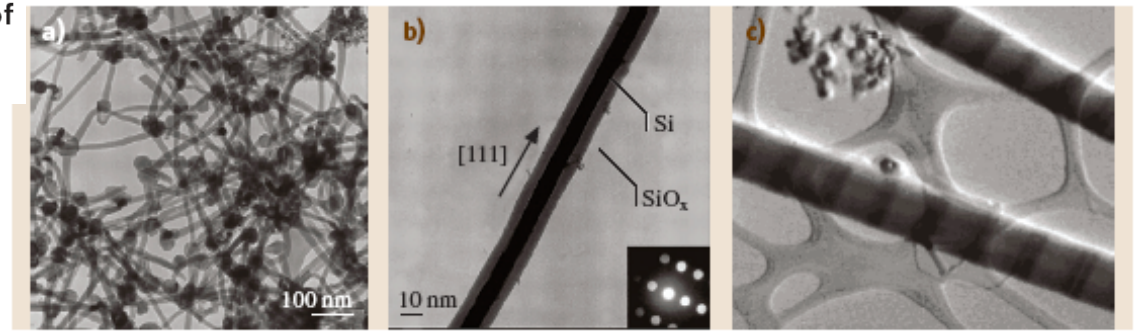

Fig. 4.6 (a) TEM images of Si nanowires produced after laser ablating a $Si_{0.9}Fe_{0.1}$ target. The dark spheres with a slightly larger diameter than the wires are solidified catalyst clusters [4.60]. (b) Diffraction contrast TEM image of a Si nanowire. The crystalline Si core appears darker than the amorphous oxide surface layer. The inset shows the convergent beam electron diffraction pattern recorded perpendicular to the wire axis, confirming the nanowire crystallinity [4.60]. (c) STEM image of $Si/Si_{1-x}Ge_x$ superlattice nanowires in the bright field mode. The scale bar is 500 nm [4.90]

630 26 JANUARY 2001 VOL 291 SCIENCE

Directed Assembly of One-Dimensional Nanostructures into Functional Networks

Yu Huang,[1]* Xiangfeng Duan,[1]* Qingqiao Wei,[1] Charles M. Lieber[1,2]†

Nanowire networks

- Alignment by flow in channels.
- Alignment on surface patterns.

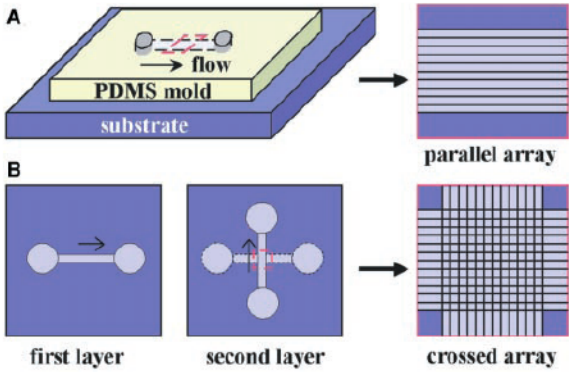

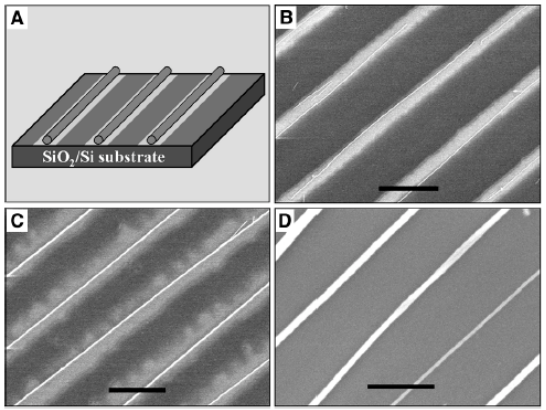

Amine terminated lines.

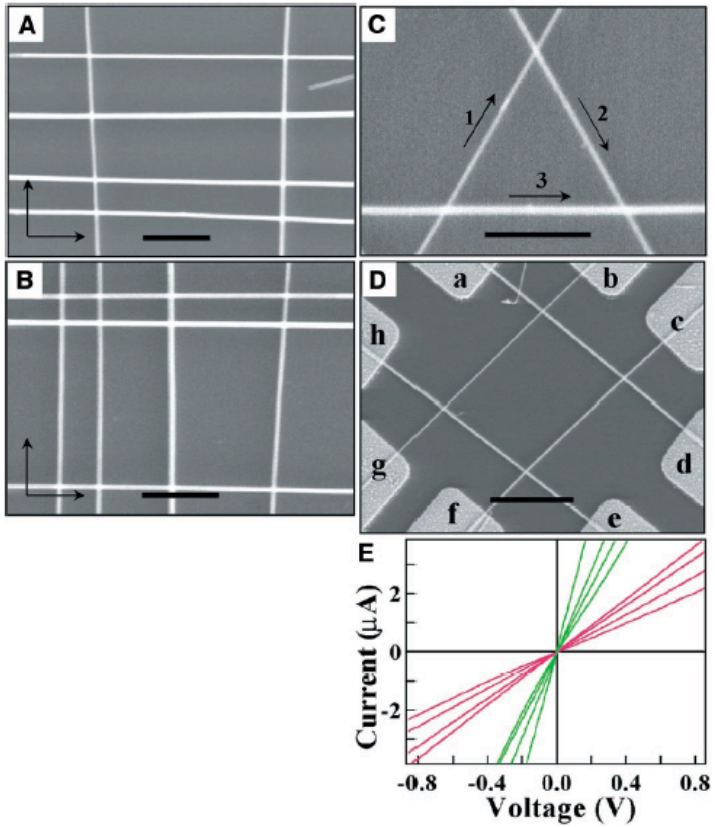

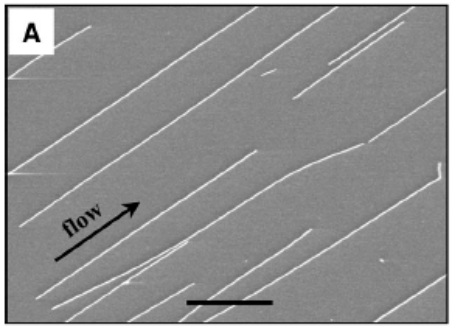

SCIENCE VOL 294 9 NOVEMBER 2001

Nanowire devices

- Doped wires, logic gates.

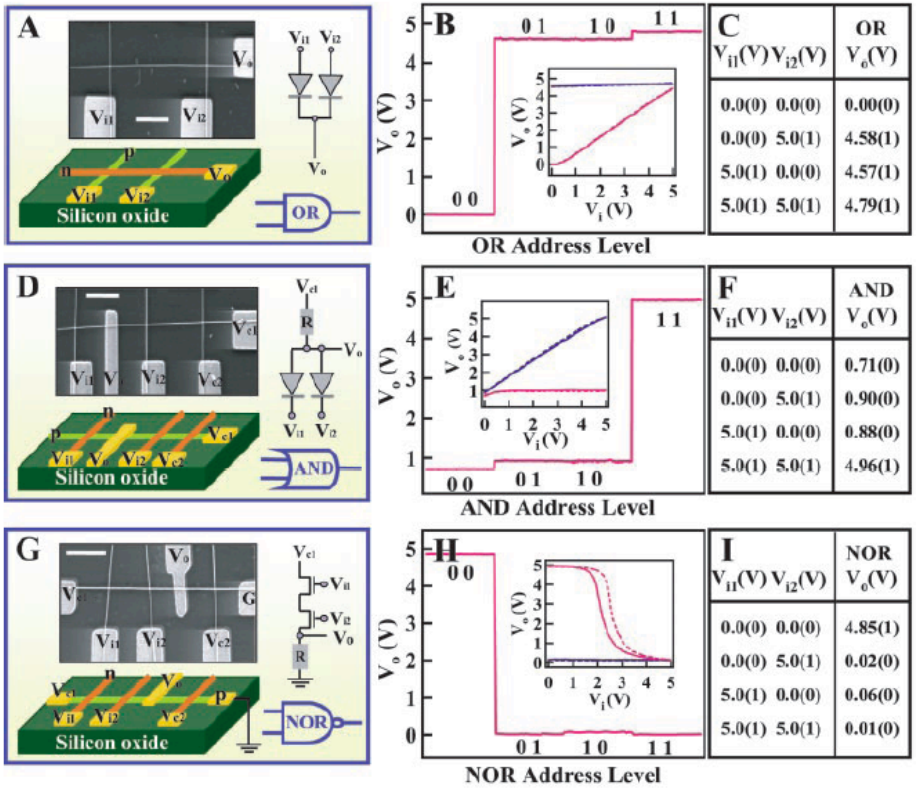

Logic Gates and Computation from Assembled Nanowire Building Blocks

Yu Huang,[1*] Xiangfeng Duan,[1*] Yi Cui,[1] Lincoln J. Lauhon,[1]
Kyoung-Ha Kim,[2] Charles M. Lieber[1,2†]

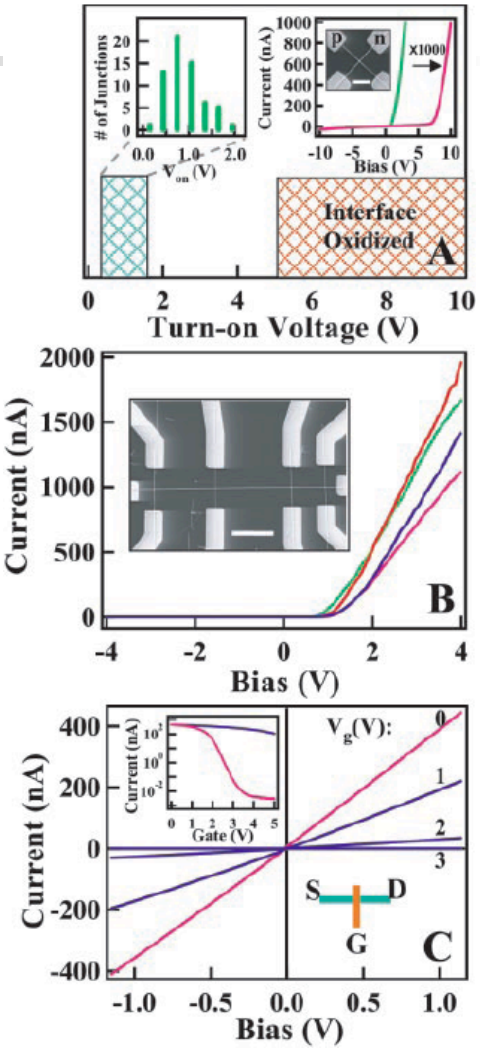

Nanowires

- More complex structures by growth.
- Organization of fully formed rods.
- Ordered growth.

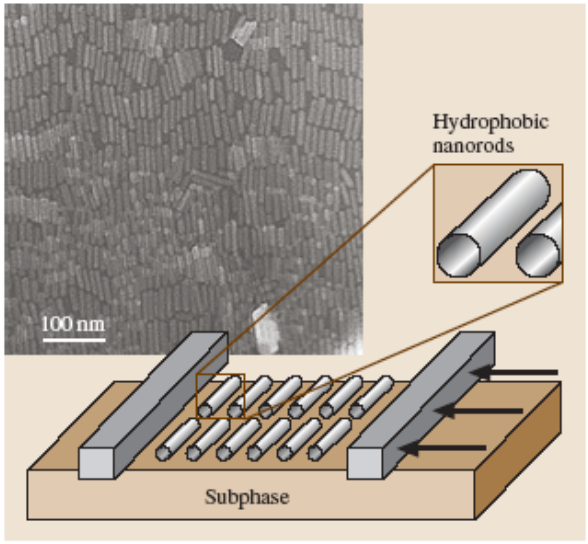

Fig. 4.10 A TEM image of a smectic phase of a $BaCrO_4$ nanorod film (*left inset*) achieved by the Langmuir–Blodgett technique, as depicted by the illustration [4.109]

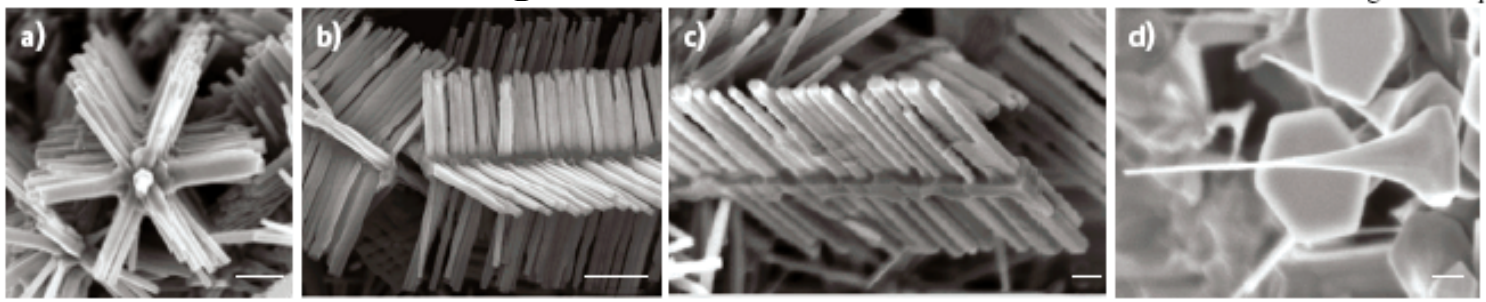

Fig. 4.9a–d SEM images of (a) 6-fold (b) 4-fold and (c) 2-fold symmetry nanobrushes made of an In_2O_3 core and ZnO nanowire brushes [4.107], and of (d) ZnO nanonails [4.108]

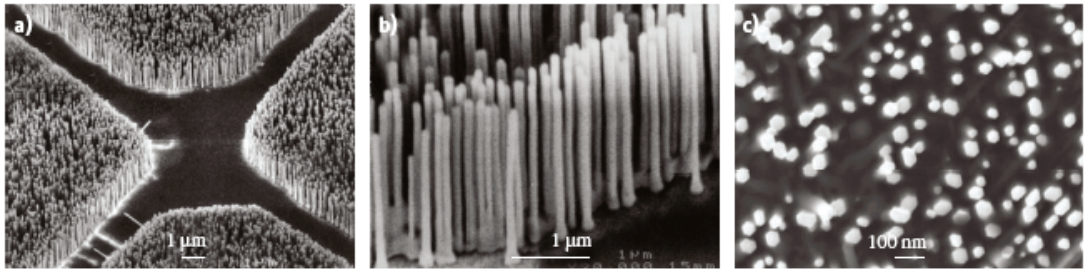

Fig. 4.11a–c SEM images of ZnO nanowire arrays grown on a sapphire substrate, where (a) shows patterned growth, (b) shows a higher resolution image of the parallel alignment of the nanowires, and (c) shows the faceted side-walls and the hexagonal cross section of the nanowires. For nanowire growth, the sapphire substrates were coated with a 1.0 to 3.5 nm thick patterned layer of Au as the catalyst, using a TEM grid as the shadow mask. These nanowires have been used for nanowire laser applications [4.115]

Nanowires

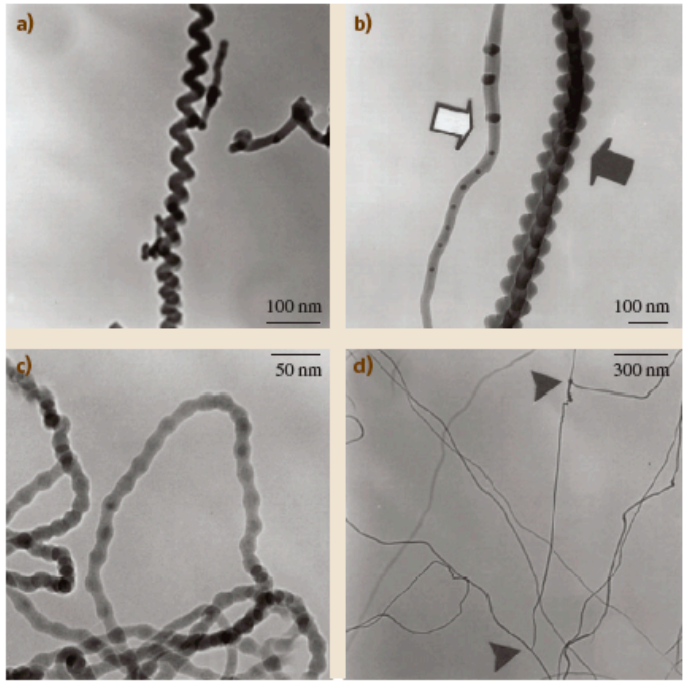

Fig. 4.13a–d TEM morphologies of four special forms of Si nanowires synthesized by the laser ablation of a Si powder target. **(a)** A spring-shaped Si nanowire; **(b)** fishbone-shaped (indicated by a *solid arrow*) and frog-egg-shaped (indicated by a *hollow arrow*) Si nanowires; and **(c)** pearl-shaped nanowires, while **(d)** shows poly-sites for the nucleation of silicon nanowires (indicated by *arrows*) [4.116]

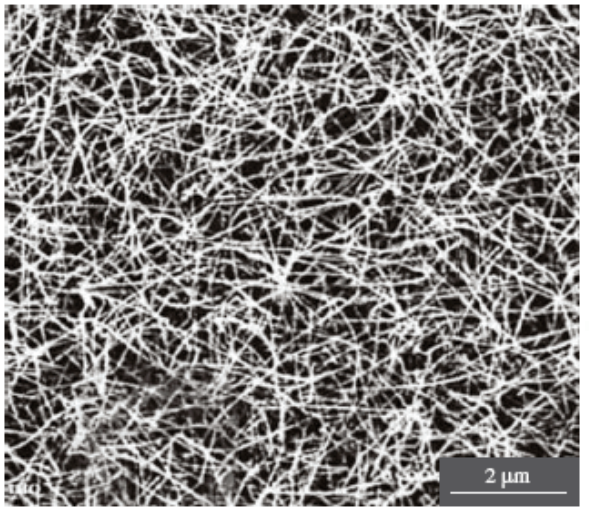

Fig. 4.12 SEM image of GaN nanowires in a mat arrangement synthesized by laser-assisted catalytic growth. The nanowires have diameters and lengths on the order of 10 nm and 10 µm, respectively [4.46]

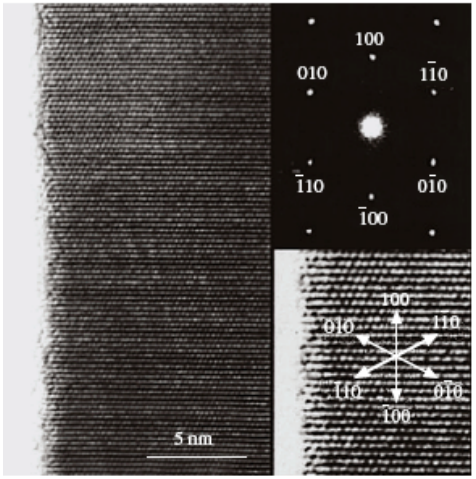

Fig. 4.14 Lattice resolved high resolution TEM image of one GaN nanowire (*left*) showing that (100) lattice planes are visible perpendicular to the wire axis. The electron diffraction pattern (*top right*) was recorded along the ⟨001⟩ zone axis. A lattice-resolved TEM image (*lower right*) highlights the continuity of the lattice up to the nanowire edge, where a thin native oxide layer is found. The directions of various crystallographic planes are indicated in the *lower right* figure [4.46]

Nanowires

- Annealing

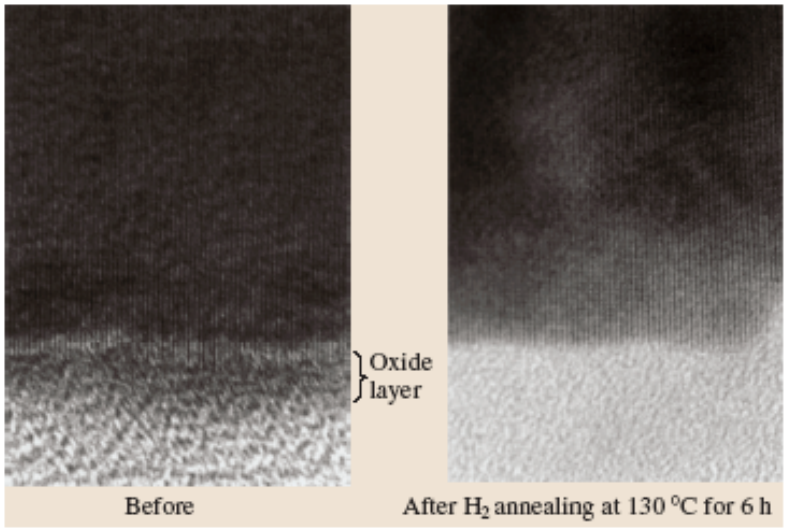

Fig. 4.16 High resolution transmission electron microscope (HRTEM) image of a Bi nanowire (*left*) before and (*right*) after annealing in hydrogen gas at 130 °C for 6 hours within the environmental chamber of the HRTEM instrument to remove the oxide surface layer [4.117]

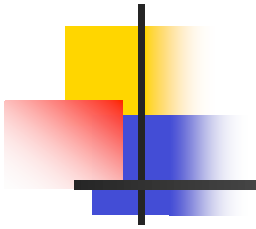

NanoParticles and Biomolecular Address Labels

- Nanoparticles, nanocrystals, nanospheres, quantum dots, etc.
- DNA (protein) conjugation.
- Self-assembly using DNA (proteins).
- Optical and electronic properties.
- Future possibilities.

Conjugation strategies

Table 1. Coupling of inorganic nanoparticles and biomolecules.

Particle	Linker	FG	Biomolecule	Reference
Au	–	HS-Cys	immunoglobulins, serum albumins	[34, 152]
Au	citrate	H_2N-Lys[a]	proteins	[156, 217]
Au	streptavidin	biotin-$(CH_2)_6$-	immunoglobulins, serum albumins	[218]
Au	**3**		immunoglobulin, streptavidin	[42]
Au	streptavidin	biotin-$(CH_2)_6$-	DNA	[148e, 219]
Au	–	HS-$(CH_2)_6$-	DNA	[77, 82]
Au	–	$(HS\text{-}PO_3R_2)_5$-	DNA	[30, 31]
Au	**2**		DNA	[33]
Au	**4**	HOOC-Glu	proteins	[43]
Au	**5**	HS-Cys	proteins	[158]
Ag	citrate	H_2N-Lys[a]	heme proteins, immunoglobulins	[35, 36, 166]
ZnS		HS-Cys	gluthathione	[47]
CdS		HS-Cys	peptides	[46]
CdS	Cd^{2+}, HS-$(CH_2)_2$-OH[a]		DNA	[39, 41]
CdSe/ZnS[b]		HS-$(CH_2)_6$-	DNA	[79]
CdSe/CdS/SiO_2[b]	**6**	NHS–biotin	streptavidin	[17]
CdSe/ZnS[b]	HS-(CH_2)-COOH	H_2N-Lys	immunoglobulin, transferrin	[18]
CdSe/ZnS[b]	**1**	H_2N-Lys[a]	leucine zipper fusion proteins	[32]
SnO_2, TiO_2	HOOC-$(CH_2)_n$-NH_2	HOOC-Glu	proteins[c]	
GaAs, InP	phosphoramide ε-NH_2	HOOC-Glu	proteins[c]	[220]

Examples of chemical interactions used for the coupling of nanoparticles with biological macromolecules (FG = functional coupling group, see Figure 3). [a] Adsorption through Coulombic interactions. [b] Core/shell nanoparticles. [c] Proposed from related studies of nanoparticle binding to analogously modified solid substrates.

C. M. Niemeyer

Angew. Chem. Int. Ed. **2001**, *40*, 4128–4158

Chemistry:

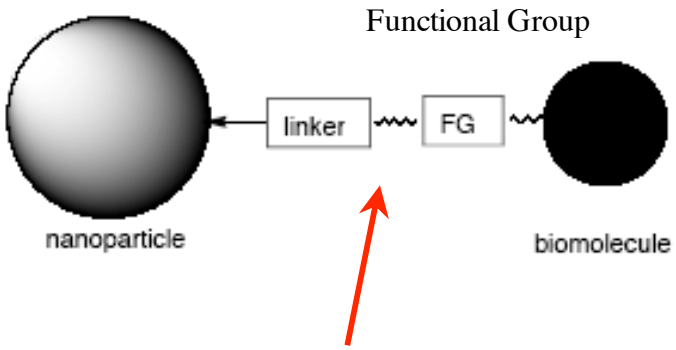

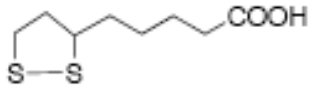

Lipoic acid

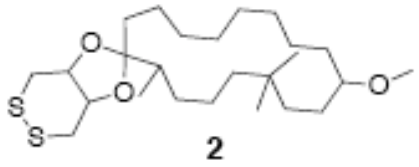

2

Cyclic disulfides

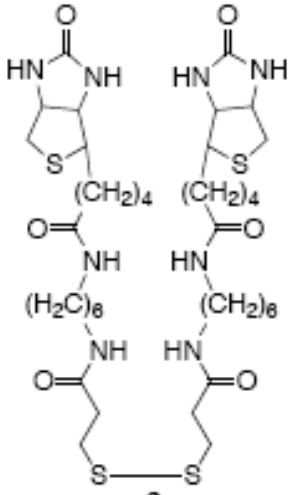

3

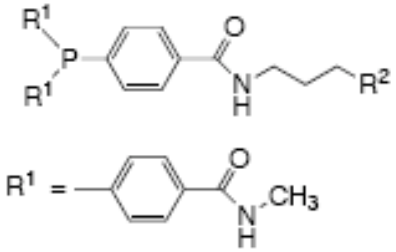

Maleimido

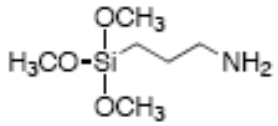

6

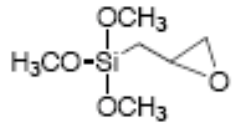

7

Silanes

Angew. Chem. Int. Ed. **2001**, *40*, 4128–4158

NP-NP

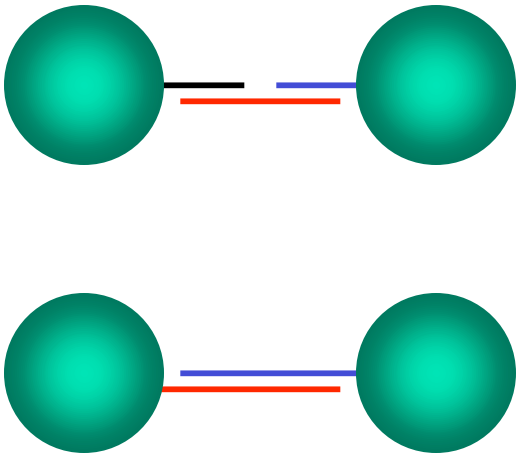

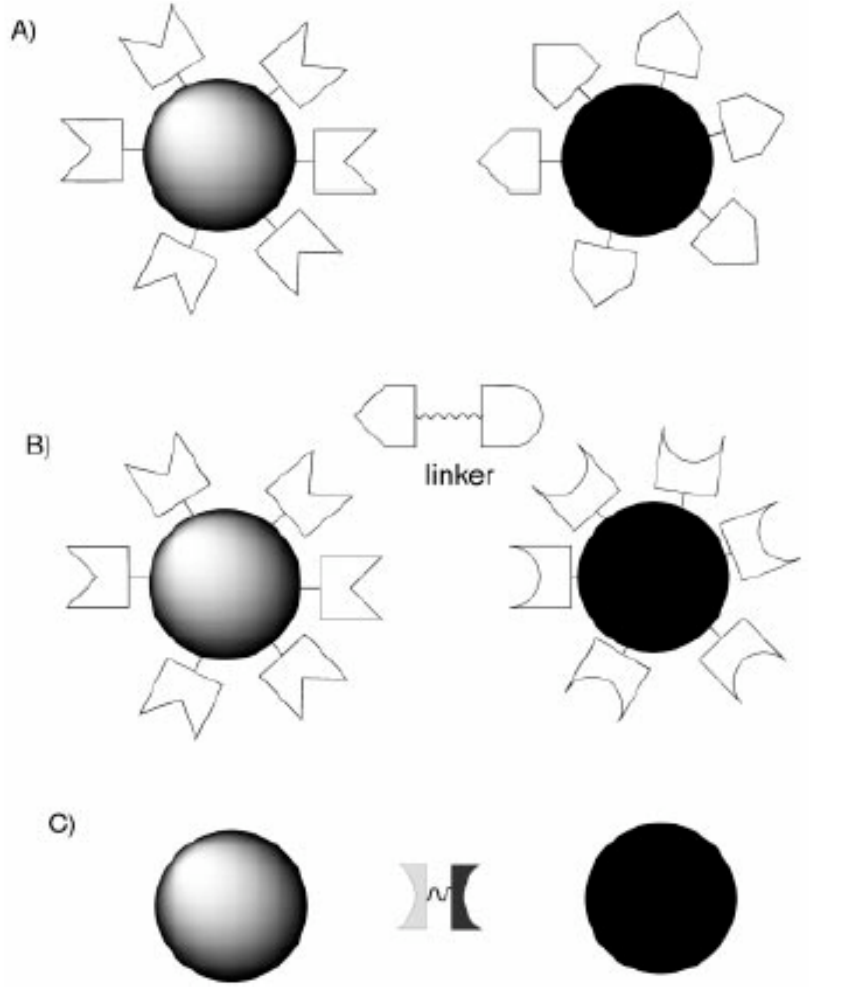

Figure 5. Solution-phase chemical coupling with biomolecular recognition elements. A) Two sets of nanoparticles are functionalized with individual recognition groups that are complementary to each other. B) The particle-bound recognition groups are not complementary to each other, but can be bridged through a bispecific linker molecule. C) A bivalent linker that directly recognizes the surfaces of the nanoparticles is used for aggregation.

Angew. Chem. Int. Ed. **2001**, *40*, 4128–4158

Simple NP-DNA Conjugates

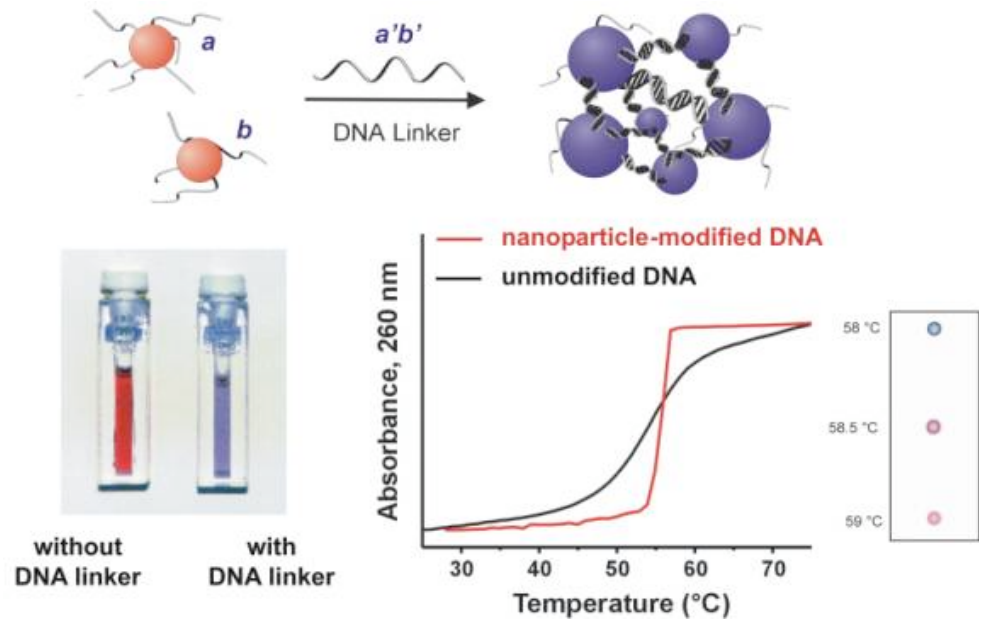

- Multiple DNA labels per NP.
- Remarkable spectroscopic changes upon DNA hybridization.
- Sharper dissociation curve.

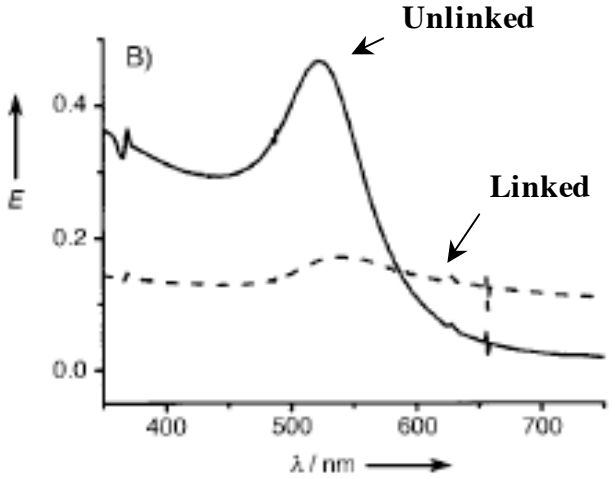

Mirkin, C. A.; Letsinger, R. L.; Mucic, R. C.; Storhoff, J. J. *Nature* **1996**, *382*, 607.

Mucic, R. C.; Storhoff, J. J.; Mirkin, C. A.; Letsinger, R. L. "DNA-Directed Synthesis of Binary Nanoparticle Network Materials," *J. Am. Chem. Soc.* **1998**, *120*, 12674-12675.

Simple NP-DNA Conjugates

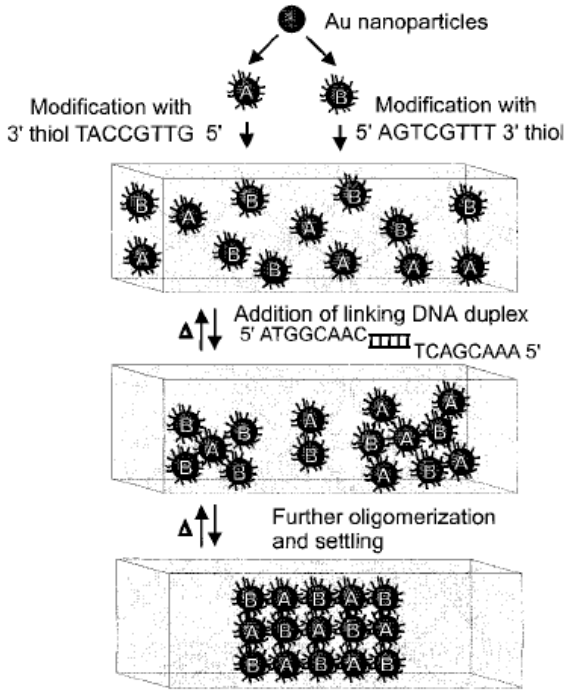

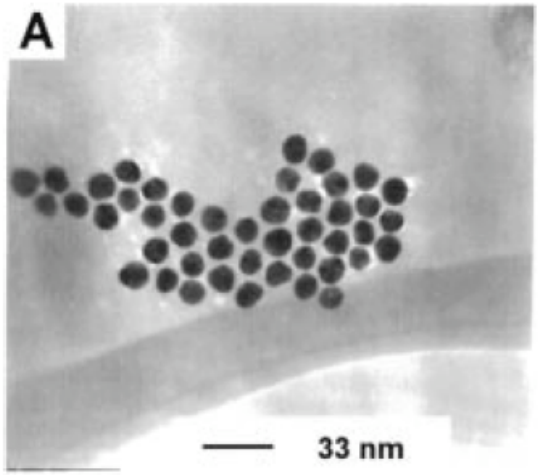

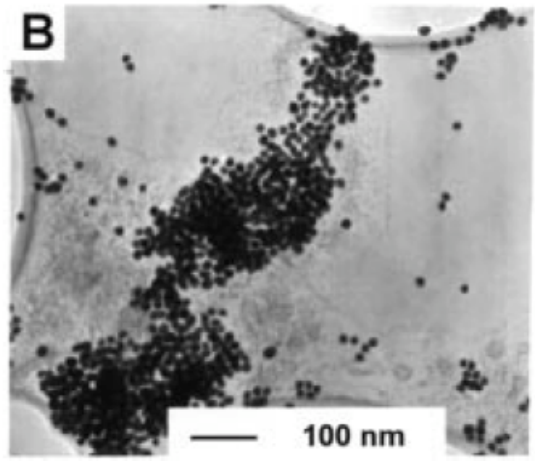

Mirkin, C. A.; Letsinger, R. L.; Mucic, R. C.; Storhoff, J. J. *Nature* **1996**, *382*, 607.

Mucic, Storhoff, Mirkin, Letsinger (1998) *JACS* **120**, 12674-12675

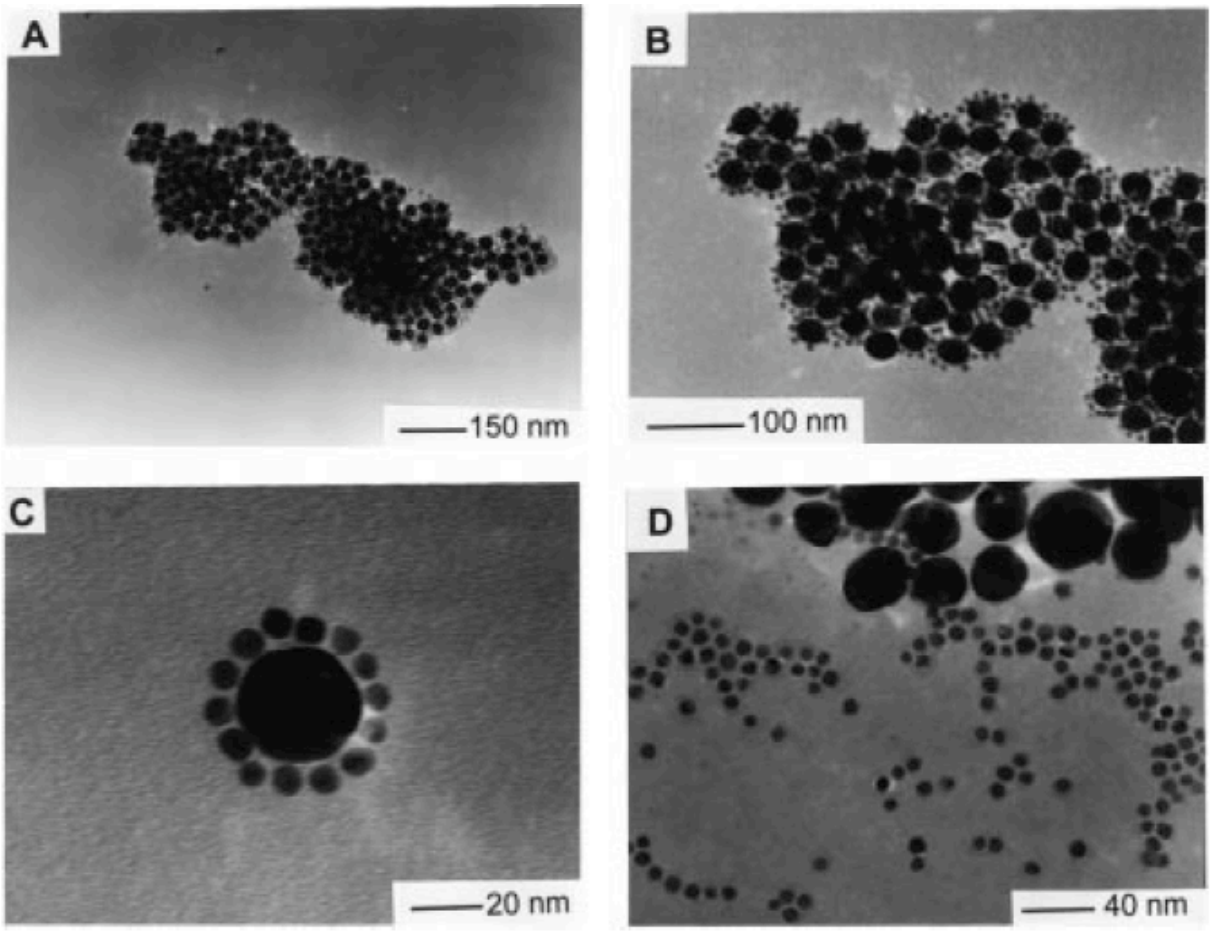

Figure 6. TEM images of binary network materials supported on holey carbon grids: (A) a DNA-linked assembly of 8 and 31 nm Au nanoparticles, (B) a smaller scale image of the DNA-linked assembly shown in A, (C) a nanoparticle "satellite structure" comprised of a 31 nm Au nanoparticle linked through DNA hybridization to several 8 nm Au nanoparticles, and (D) a control experiment containing 8 and 31 nm diameter Au nanoparticles without DNA linker, which exhibits significant particle phase segregation. (Reprinted with permission from ref 6. Copyright 1998 American Chemical Society.)

DNA-Based Assembly of Gold Nanocrystals**

Colin J. Loweth, W. Brett Caldwell, Xiaogang Peng,
A. Paul Alivisatos,* and Peter G. Schultz*

Angew. Chem. Int. Ed. **1999**, *38*, No. 12

- 1:1 DNA:nanoparticle conjugates purified by PAGE.
- Au NP stablized with dipotassium bis(p-sulfonatophenyl)phenylphosphane dihydrate.
- Binary and ternary complexes made.

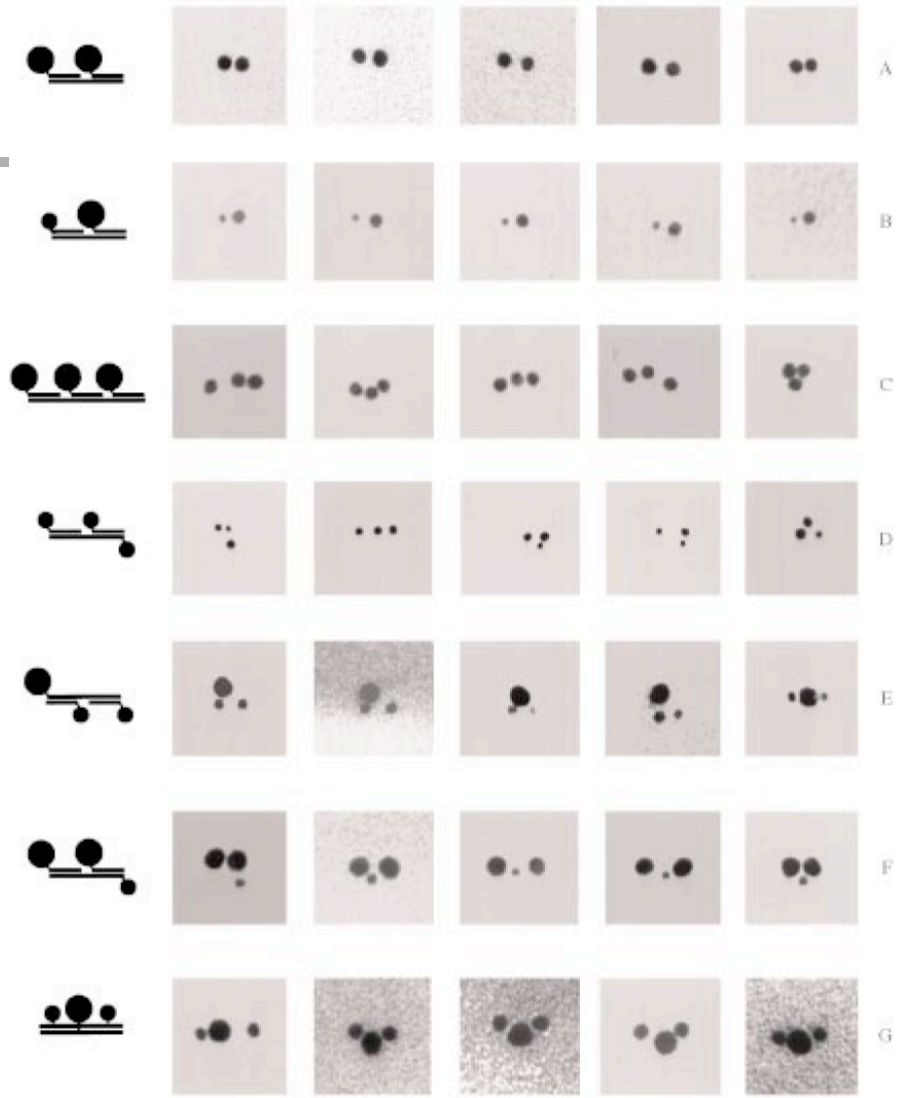

Undecagold

- 11 gold atoms
- < 1 nm diameter
- monofunctional

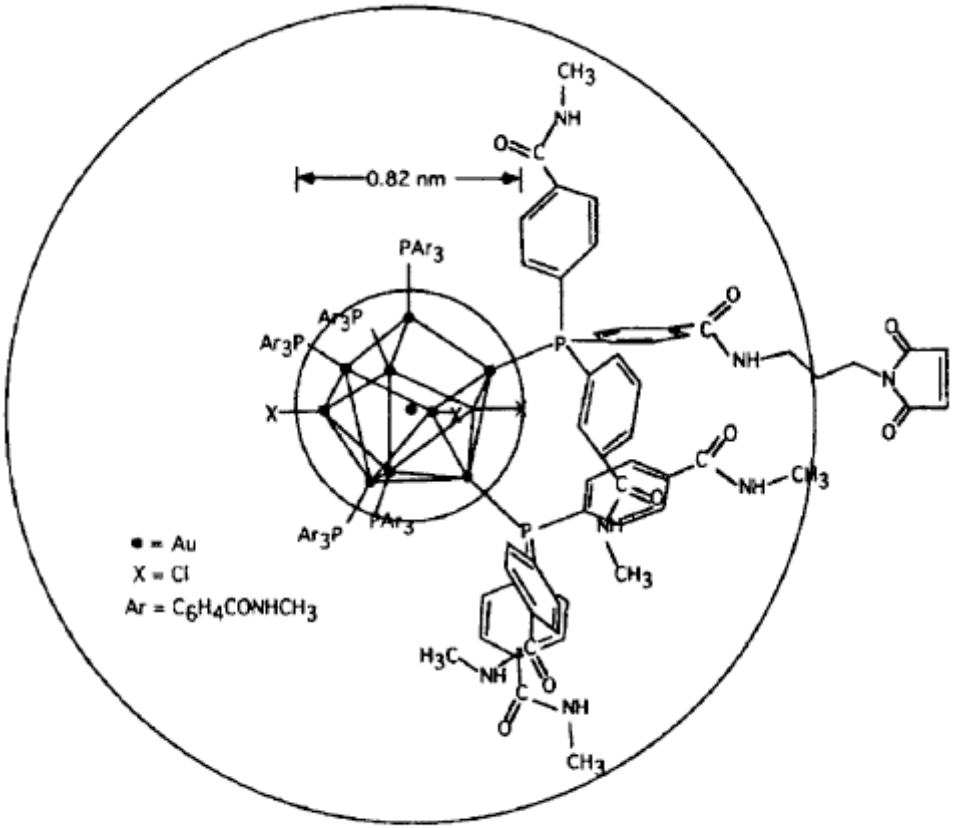

Figure 4. Molecular structure of an undecagold cluster, which is stabilized with phosphane ligands. A single maleimido group is attached per gold cluster to allow chemical coupling of thiolated components. Reproduced from http://www.nanoprobes.com.

NP networks

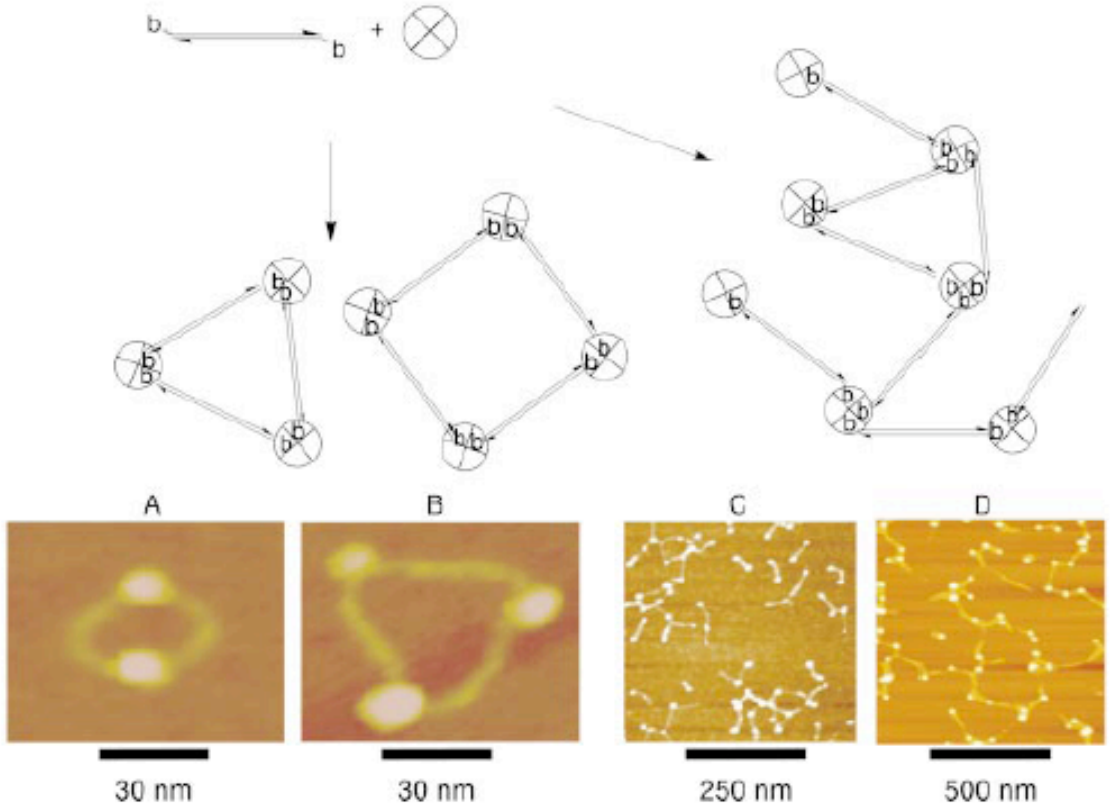

Figure 10. Synthesis of nanoparticle networks by using dsDNA as spacer groups. The dsDNA fragments contain two binding sites (b) attached to the two 5′-ends of the dsDNA. The binding sites are either biotinyl groups that allow cross-linking of the biotin-binding protein streptavidin as a model nanoparticle (A – C), or thiol groups that allow the connection of 5-nm gold colloids (D). Adapted in part from reference [86], with permission.

C. M. Niemeyer, M. Adler, S. Lenhert, S. Gao, H. Fuchs, L. F. Chi, *ChemBioChem* **2001**, *2*, 260 – 265.

Directed Assembly of Periodic Materials from Protein and Oligonucleotide-Modified Nanoparticle Building Blocks**

So-Jung Park, Anne A. Lazarides, Chad A. Mirkin,* and Robert L. Letsinger*

Angew. Chem. Int. Ed. **2001**, *40*, No. 15 2909-2912

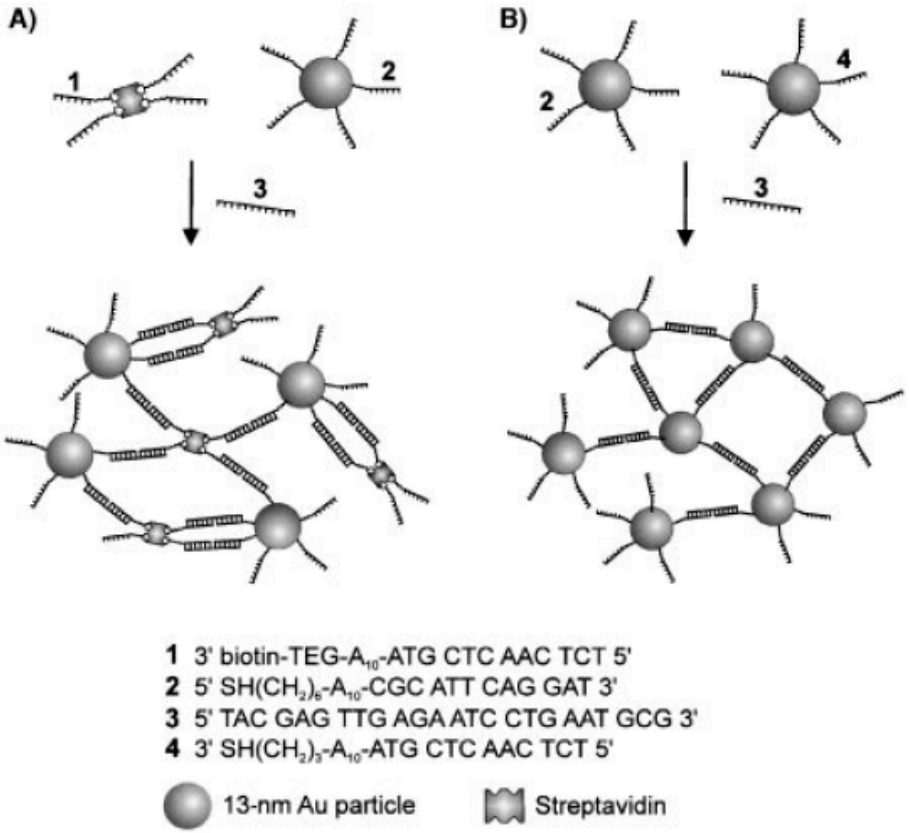

Figure 1. Schematic representation of DNA-directed assembly of Au nanoparticles and streptavidin. A) Assembly of oligonucleotide-functionalized streptavidin and Au nanoparticles (Au–STV assembly). B) Assembly of oligonucleotide-functionalized Au nanoparticles (Au–Au assembly). Note that **1** and **4** have the same DNA sequence.

Journal of Nanoparticle Research **4:** 313–317, 2002.

Selfassembly of metallic nanoparticle arrays by DNA scaffolding

Shoujun Xiao[1,2], Furong Liu[3], Abbey E. Rosen[2], James F. Hainfeld[4], Nadrian C. Seeman[3], Karin Musier-Forsyth[2] and Richard A. Kiehl[1,*]

[1]*Electrical and Computer Engineering Department,* [2]*Chemistry Department, University of Minnesota, Minneapolis, MN 55455, USA;* [3]*Chemistry Department, New York University, New York, NY 10003, USA;* [4]*Biology Department, Brookhaven National Laboratory, Upton, NY 11973, USA;*

**Author for correspondence (E-mail: kiehl@ece.umn.edu)*

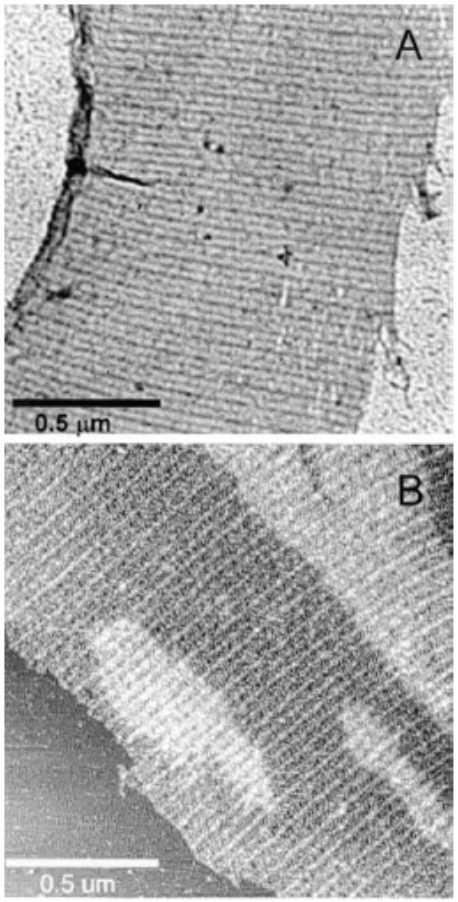

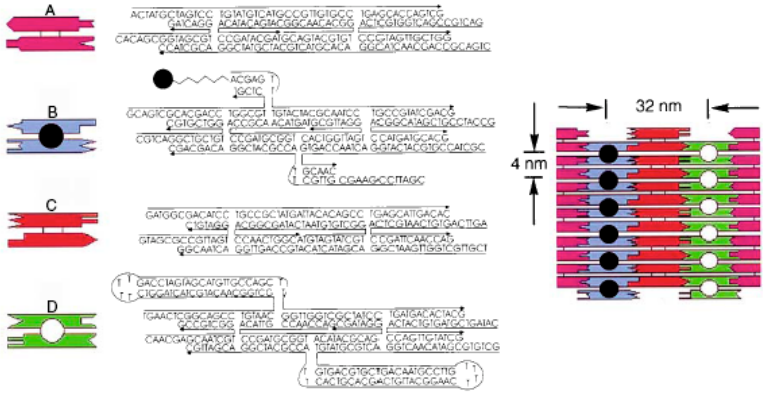

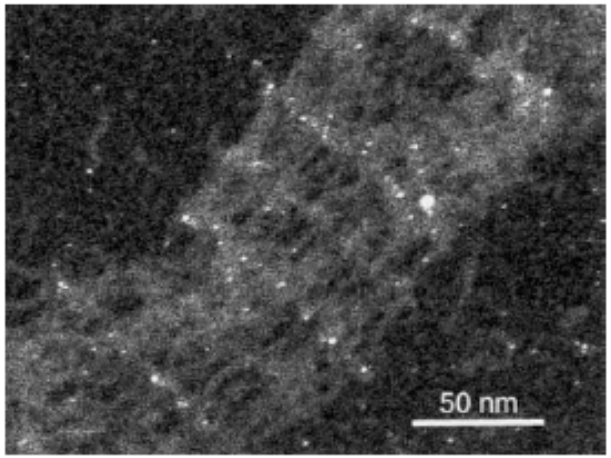

Figure 4. Scanning TEM image of a DNA crystal incorporating the DNA–Au conjugate.

LaBean

Organization of Streptavidin and Gold with TAE Linear Assembly

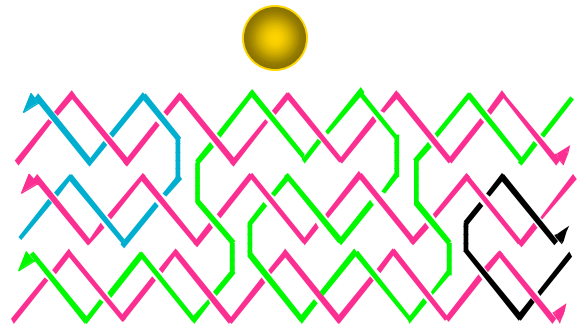

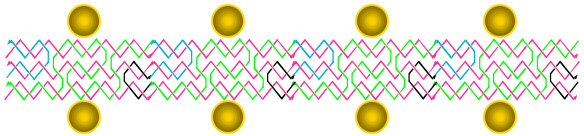

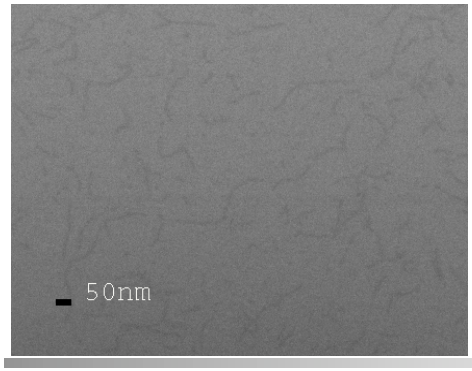

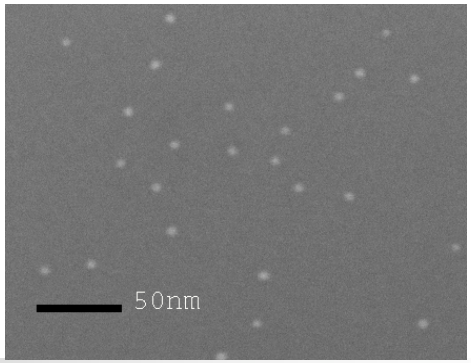

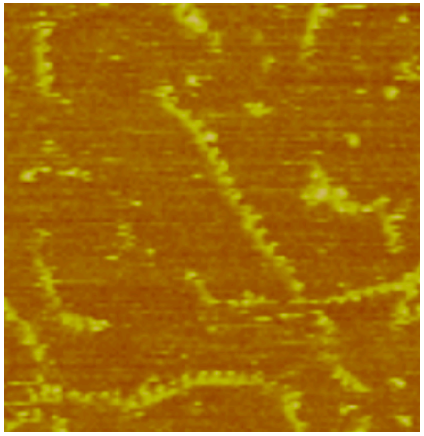

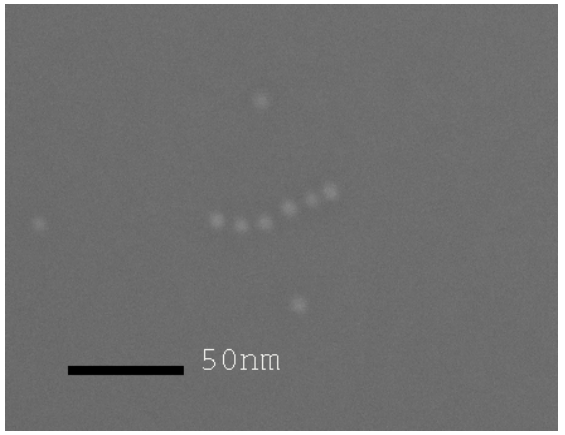

500x500 nm

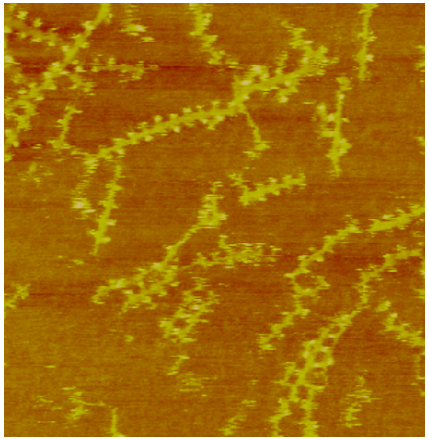

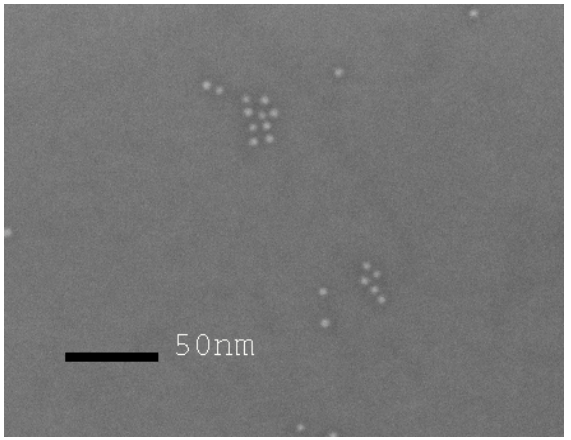

500x500 nm

H. Li, S- H. Park, J. H. Reif, T. H. LaBean, and Hao Yan, (2004) DNA Templated Self-Assembly of Protein and Nanoparticle Linear Arrays, *J. Am. Chem. Soc.* **126**, 418-419.

DNA Lattice Patterned 2D Nanoparticle Arrays

- Nanoparticle/oligonucleotide conjugate (1:1)
- 4x4 Tile array.
- Research challenge: compatible conditions for solubility and assembly.

A(5nm Gold)

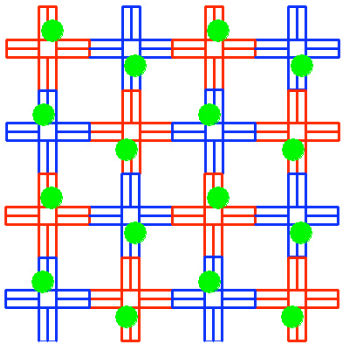

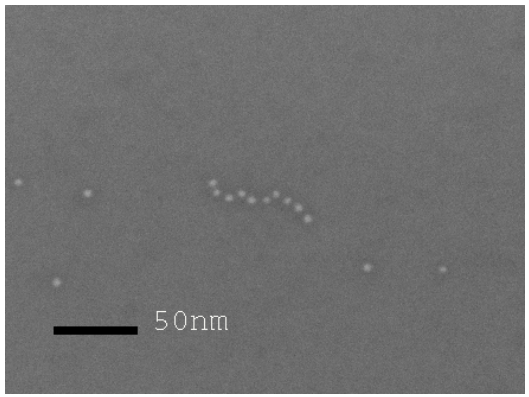

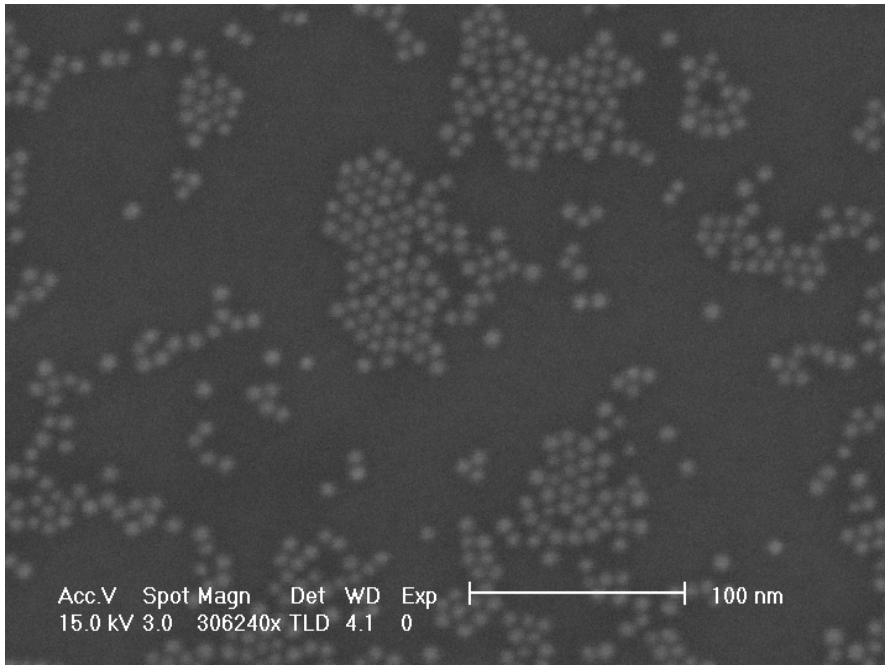

H. Li, S- H. Park, J. H. Reif, T. H. LaBean, and Hao Yan, (2004) DNA Templated Self-Assembly of Protein and Nanoparticle Linear Arrays, *J. Am. Chem. Soc.* **126**, 418-419.

Remote electronic control of DNA hybridization through inductive coupling to an attached metal nanocrystal antenna

NATURE | VOL 415 | 10 JANUARY 2002 | 152-155

Kimberly Hamad-Schifferli*, John J. Schwartz†, Aaron T. Santos*, Shuguang Zhang‡ & Joseph M. Jacobson*

** The Media Laboratory and the ‡Center for Biomedical Engineering, Massachusetts Institute of Technology, 77 Massachusetts Ave., Cambridge, Massachusetts 02139, USA*

Here we demonstrate remote electronic control over the hybridization behavior of DNA molecules, by inductive coupling of a radio-frequency magnetic field to a metal nanocrystal covalently linked to DNA15. Inductive coupling to the nanocrystal increases the local temperature of the bound DNA, thereby inducing denaturation while leaving surrounding molecules relatively unaffected. Moreover, because dissolved biomolecules dissipate heat in less than 50 picoseconds, the switching is fully reversible.

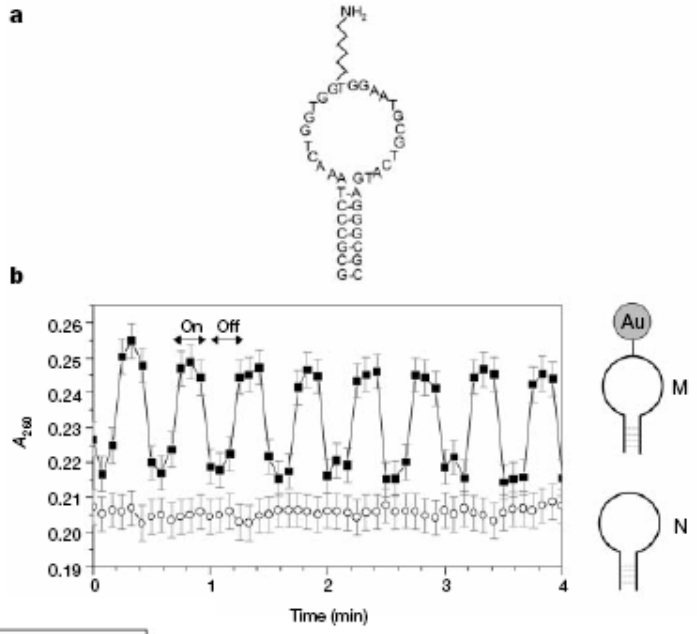

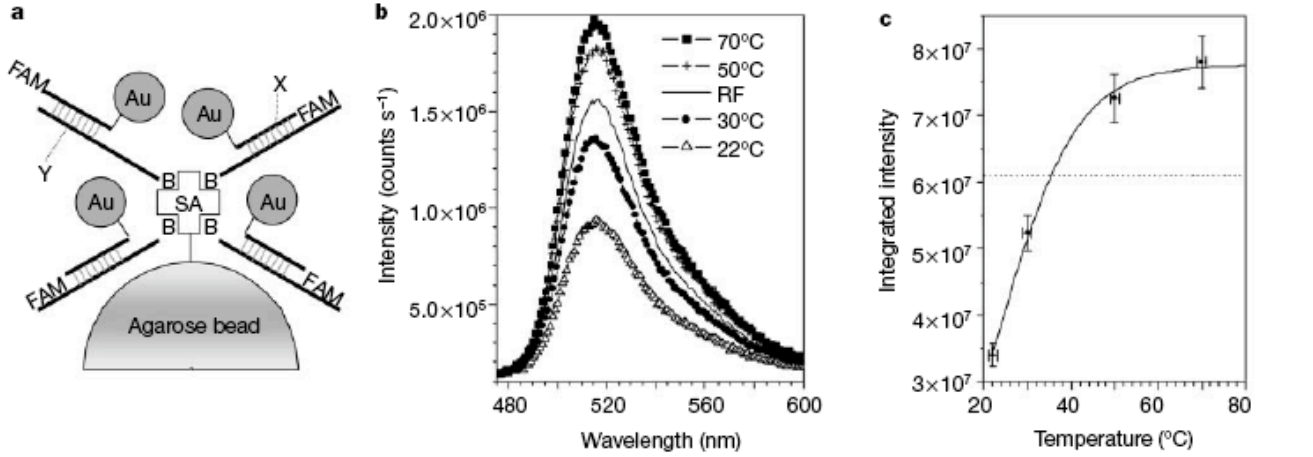

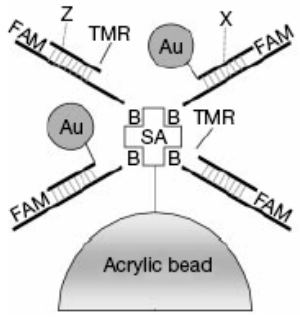

Figure 2 Determination of effective temperature from inductive coupling to a gold nanocrystal linked to DNA. **a**, The two-phase system. X is a 12-nucleotide DNA molecule covalently labelled with a gold nanocrystal on its 3′ end and the fluorophore FAM on its 5′ end. Its complementary strand Y has biotin (B) on the 5′ end, which was captured onto agarose beads with streptavidin (SA) on the surface. Once X dehybridizes from Y it can diffuse into the supernatant. **b**, Supernatant fluorescence spectra. Each sample is subject to a fixed temperature (22 °C, 30 °C, 50 °C, 70 °C) or RFMF (solid line). **c**, Integrated peak intensity of the supernatant fluorescence spectra shown in **b** (circles) and a sigmoidal fit (solid line), and the intensity of the sample exposed to RFMF (dotted line). Extrapolation of RFMF sample intensity results in an effective temperature of 35 °C for X.

49 GHz = optimal
1 GHz used

Nanowires as Building Blocks for Self-Assembling Logic and Memory Circuits

Nina I. Kovtyukhova[a, b] and Thomas E. Mallouk*[a]

Chem. Eur. J. **2002**, *8*, No. 19 4354-4363

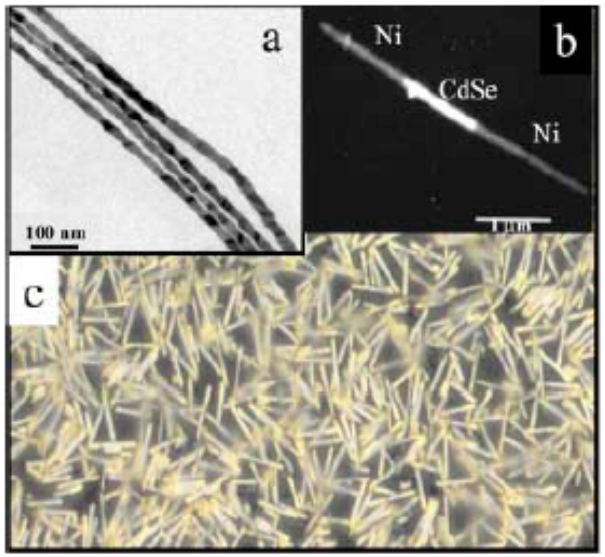

Figure 2. Electron micrographs of a) 20 nm diameter gold wires grown in polycarbonate membranes, and b) a 70 nm diameter Ni-CdSe-Ni wire grown in polycarbonate. An optical micrograph of 350 nm diameter Au-Pt-Au wires is shown in c).

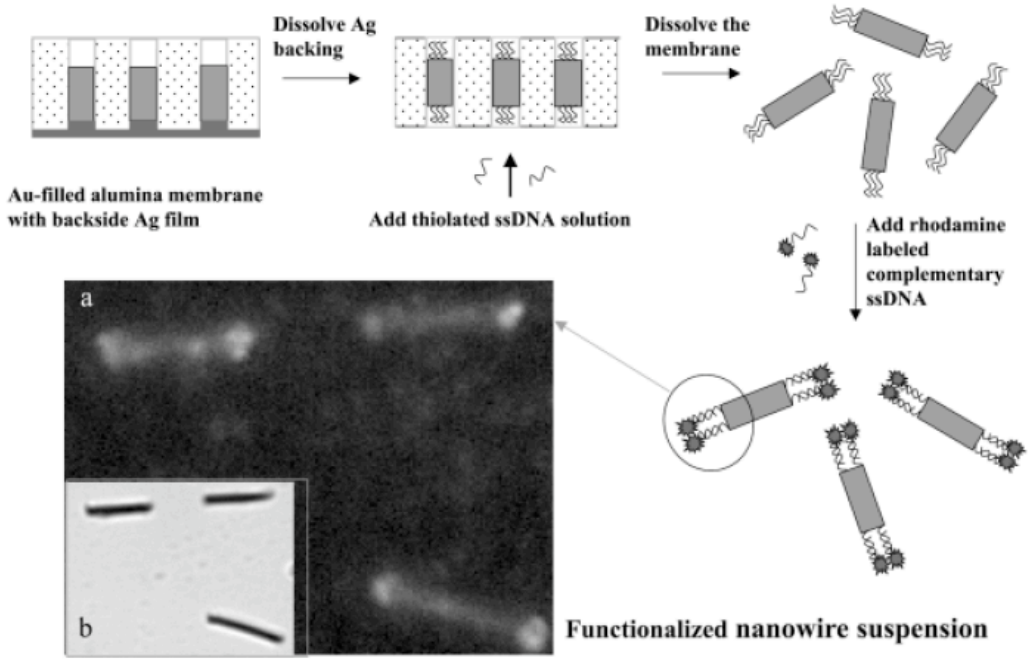

Figure 6. Scheme for in-membrane derivatization of the tips of gold nanowires with thiolated ssDNA. The nanowires are released into solution and then treated with rhodamine-labeled complementary ssDNA, which makes their tips fluorescent. a) Fluorescence and b) bright field micrographs of 350 nm diameter gold wires derivatized according to the scheme.

Metallic nanowires offer more control of surface chemistry, length, diameter, and transport properties compared to CNT or semiconductor nanowires.

Chem. Eur. J. **2002**, *8*, No. 19 4354-4363

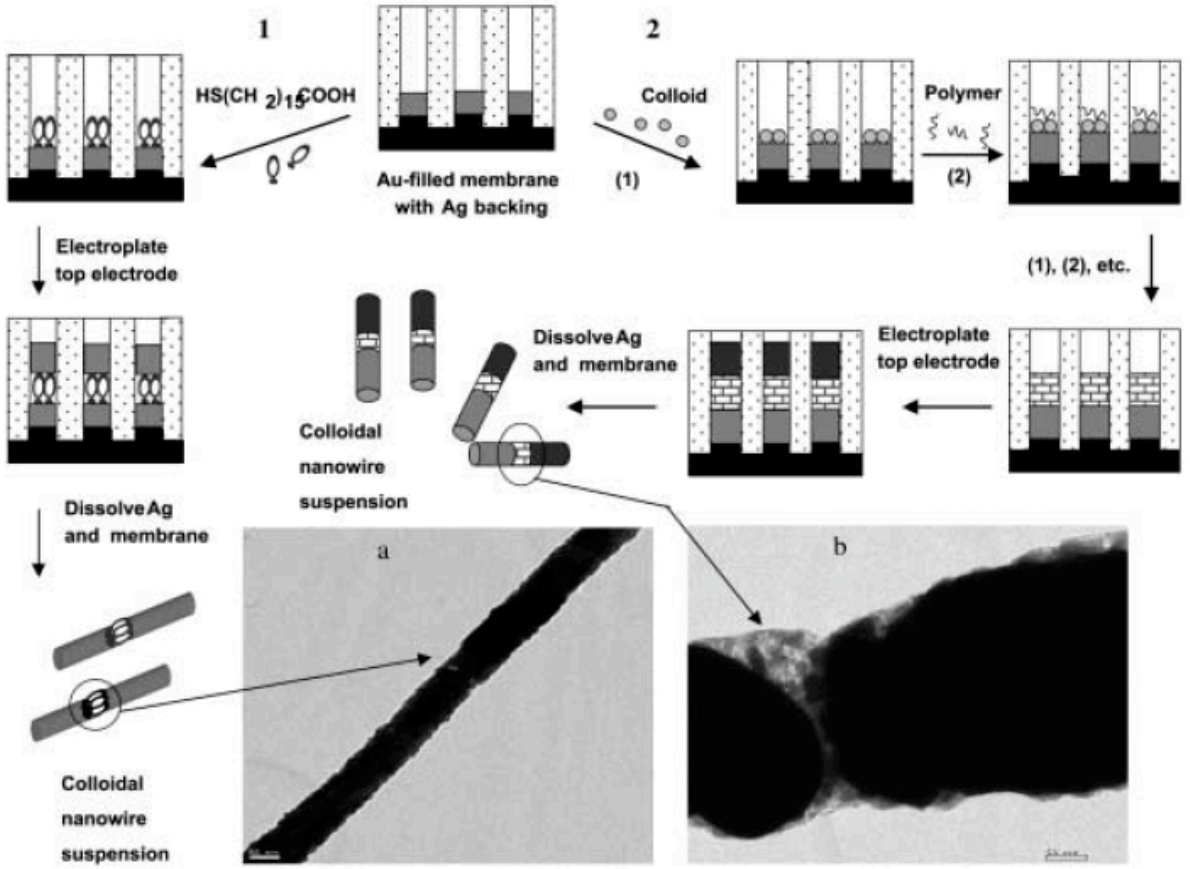

Figure 7. Top: Scheme for preparing in-wire devices by: 1) self-assembly of a MHDA monolayer, or 2) layer-by-layer assembly of TiO_2/PSS multilayer film on the exposed tip of a bottom metal electrode, followed by electroless seeding and electroplating of a top metal electrode. Bottom: TEM images of an as-prepared a) Au/$S(CH_2)_{15}COOH$/Au device, and b) a $Ag(TiO_2/PSS)_9TiO_2$/Au device. In b), electron beam-induced melting of the junction allows one to visualize the junction.

Chem. Eur. J. **2002**, *8*, No. 19 4354-4363

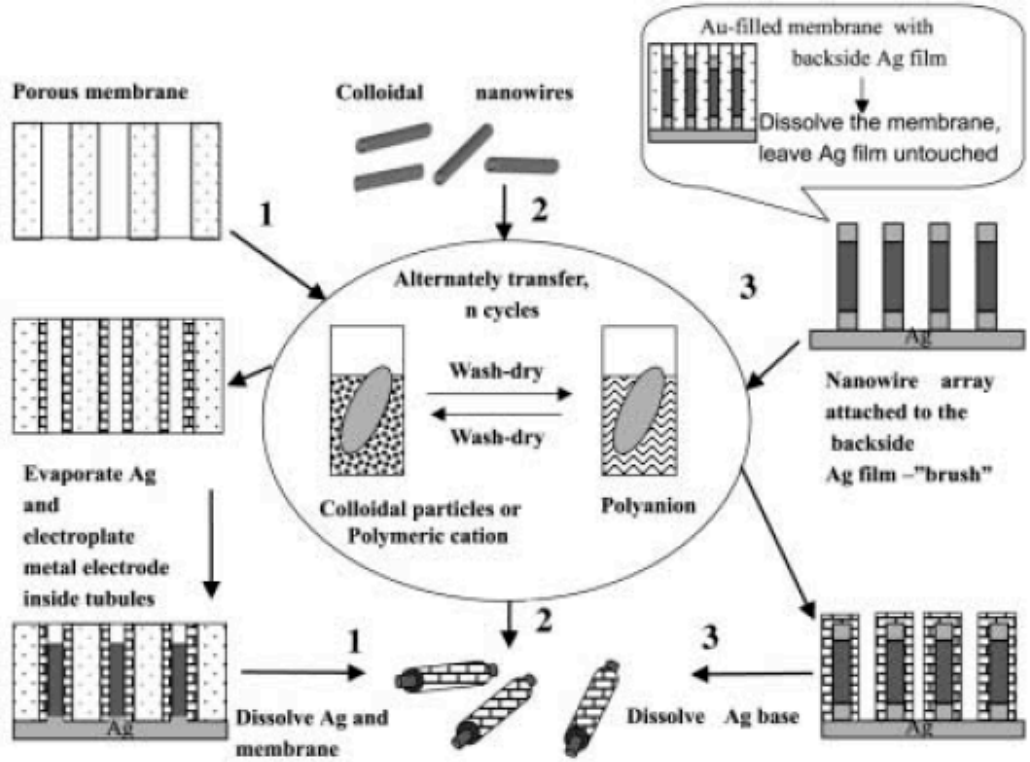

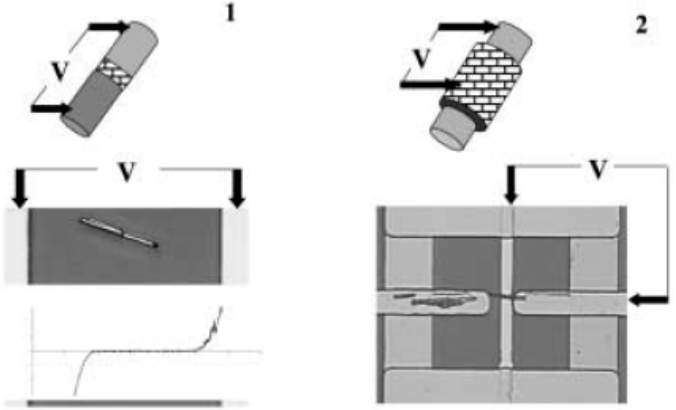

NP biosensor

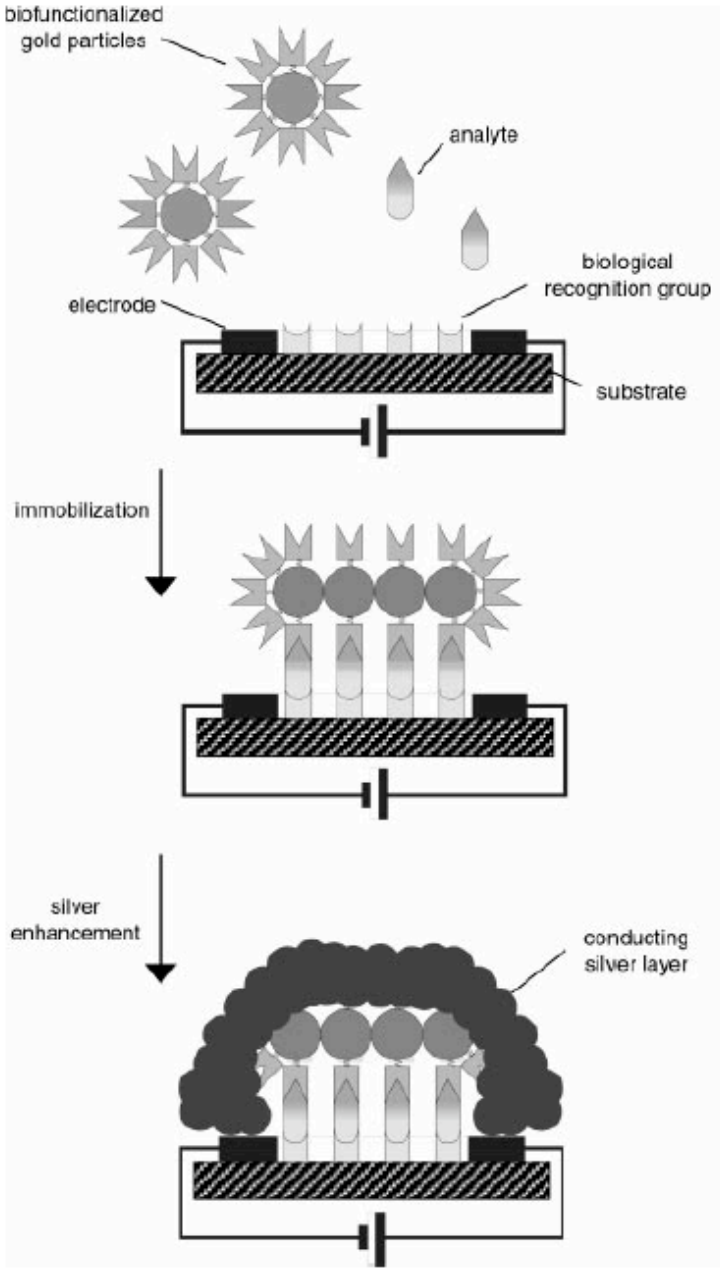

Figure 20. Electrical detection of biorecognition processes. Receptor groups such as antibodies or DNA oligomers are immobilized in the gap between two microelectrodes and used as a capture agent to bind complementary target molecules specifically. In a sandwich-type assay, the captured analyte is tagged with colloidal gold by a second biological recognition unit. Subsequent reductive deposition of silver leads to the formation of a conducting metal layer which short-circuits the two electrodes.

C. M. Niemeyer

Angew. Chem. Int. Ed. **2001**, *40*, 4128–4158